Received: 30 October 2023 | Revised: 4 April 2024 | Accepted: 3 May 2024

DOI: 10.1002/joc.8487

RESEARCH ARTICLE

International Journal of Climatology RMetS

Trends in temperature and precipitation at high and low elevations in the main mountain ranges of the Iberian Peninsula (1894–2020): The Sierra Nevada and the Pyrenees

Javier Sigro[1] | **Mercè Cisneros**[1,2] | **Antonio J. Perez-Luque**[3] | **Carmen Perez-Martinez**[3] | **Teresa Vegas-Vilarrubia**[4]

[1]Centre for Climate Change, Research Institute in Sustainability, Climate Change and Energy Transition (IU-RESCAT), Universitat Rovira i Virgili, Tarragona, Spain

[2]CRG Marine Geosciences, Department of Earth and Ocean Dynamics, Faculty of Earth Sciences, University of Barcelona, Barcelona, Spain

[3]Department of Ecology and Institute of Water Research, University of Granada, Granada, Spain

[4]Department of Evolutionary Biology, Ecology and Environmental Sciences, University of Barcelona, Barcelona, Spain

Correspondence
Javier Sigro, Centre for Climate Change, Research Institute in Sustainability, Climate Change and Energy Transition (IU-RESCAT), Universitat Rovira i Virgili, Tarragona, Spain.
Email: javier.sigro@urv.cat

Funding information
Ministry for the Ecological Transition and the Demographic Challenge of Spain, Grant/Award Number: OAPN-2476-S/2017; "European Union NextGenerationEU/PRTR" with a "Juan de la Cierva" fellowship programme, Grant/Award Number: JDC2022-050056-I

Abstract

This study describes temperature and precipitation trends in the two National Parks located in the two highest mountain ranges on the Iberian Peninsula: the Sierra Nevada (Sierra Nevada National Park, SN) and the Pyrenees (Aigüestortes i Sant Maurici National Park, ASM). Special focus is placed on analysing disparities between the lowlands and the highlands, as well as the agreement between observational data and grid data (IBERIA01 and E-OBS). For this purpose, a quality-controlled and homogeneity-adjusted database of the daily maximum temperature, minimum temperature and precipitation (SMADS database) has been generated. Regional trends in mean temperature indicate that warming in ASM (0.17°C·decade^{-1}) was greater than in the Sierra Nevada (SN) (0.13°C·decade^{-1}) in the longest joint period, 1930–2020. For annual precipitation, the trends over the past nine decades were negative, although not significantly. Only the summer in SN showed a significant negative trend, which has intensified in recent decades to −13.4%·decade^{-1} for 1975–2020. A parallel evolution was observed in the annual mean temperature of the highlands (>1500 m) and lowlands (<1500 m) of ASM, with a common trend of 0.17°C·decade^{-1}, while in SN negative elevation-dependent warming was detected. Differences between lowlands and highlands were also noted in precipitation trends in both mountain ranges: a positive trend in precipitation was found in the lowlands while in the highlands practically null trends (ASM) or decreasing precipitation trends (SN) were detected. The comparison of the Spanish Mountain Adjusted Daily Series (SMADS) results with the IBERIA01 and E-OBS grid series yielded differences no greater than

±0.2°C·decade^{-1}. No notable differences were detected between the regional trends calculated with observational series or with grid series. These results worsened when the differences in the trends detected in the individual observed temperature series were compared against the corresponding grid series.

KEYWORDS

climate variability, mountain climates, precipitation, Spain, temperature, trends

1 | INTRODUCTION

High mountain regions share common features, including rugged terrain, a low-temperature climate regime, steep slopes and institutional and spatial remoteness (IPCC, 2022). Due to their higher elevation compared with the surrounding landscape, mountains often feature cryosphere components, such as glaciers, snow cover and permafrost, which significantly influence bordering lowland areas, including those located far from the mountains (Huggel et al., 2015). The mountains act as the main store of fresh water for many of the world's major river basins. The presence of solid water in the mountains plays a fundamental role in the regulation of the river flows (Bradley et al., 2006; Viviroli et al., 2011) on which an increasing number of people depend (Viviroli et al., 2020).

Climate change does not affect all regions equally: the warming rate can differ from area to area (Gulev et al., 2023), with mountain ranges being particularly vulnerable (Hock et al., 2019). In recent decades, several studies have examined the evolution of temperature signals in mountain areas across the world (Diaz & Bradley, 1997; Pepin & Lundquist, 2008; Pepin et al., 2022; Qixiang et al., 2018; Wang et al., 2016a; Zeng et al., 2015), consistently revealing significant trends towards temperature increases. Long-term studies have discovered positive temperature trends in European mountain areas during the last century which have become more intense in recent decades. For instance, in the Alps, Europe's most extensive mountain range, sustained temperature increases have been detected since the 19th century with trends of around 0.12°C·decade^{-1} (Auer et al., 2007; Begert & Frei, 2018). In more recent periods, the trends have become more pronounced, especially after the 1970s, with increases of around 0.3°C·decade^{-1} in the last 60 years (Ceppi et al., 2012; Lejeune et al., 2019; Ohmura, 2012). Precipitation trends, meanwhile, vary between positive in the mountain areas of northern Europe (Irannezhad et al., 2017) and negative (−1.8%·decade^{-1}) in the area of the Alps and in Italy (Masson & Frei, 2016; Scorzini & Leopardi, 2019).

Many studies have suggested that mountain warming rates are not homogeneous and are elevation-dependent (Diaz & Bradley, 1997; Pepin et al., 2015; Qixiang et al., 2018; Rangwala & Miller, 2012; Vuille & Bradley, 2000), related to various physical mechanisms that determine the evolution of local effects on a climatological scale, such as snow albedo, atmospheric moisture, thermal emission, aerosols and clouds. Elevation-dependent warming (EDW) does not always imply that warming is more rapid in mountains than in lowlands, but rather that there is a systematic difference in warming rates based on elevation. Initially, higher warming rates were detected in highlands than in lowlands in locations across the world (Diaz & Bradley, 1997; Qixiang et al., 2018; Wang et al., 2016a; Zeng et al., 2015), but closer examination of regional mountain/lowland studies reveals no systematic difference in warming rates in high- versus low-elevation groups (Pepin et al., 2022).

Similar to temperature, the evolving interaction between synoptic flow and orographically induced circulations can cause significant variations in the distribution of precipitation on climatological time scales (Shi & Durran, 2014). Precipitation changes based on station data are inconsistent and, to our knowledge, no systematic comparison between mountain and lowland precipitation trends has yet been conducted. Gridded datasets show that mountain precipitation increases are weaker than for lower elevations worldwide, which points to the reduced elevation-dependency of precipitation, especially in midlatitudes (Pepin et al., 2022).

Gridded datasets that enable the analysis of climatic variables are commonly used in climate research as they provide stable, continuous, and spatially homogeneous signals. This has led to their widespread application in the analysis of climate variability and trends in all types of terrains, including those with poor observation station coverage. Notwithstanding, the ability to reliably represent the behaviour of these climatic variables depends to a certain extent on the density of the stations that provide the base data, the topography of the terrain and the algorithms used to carry out the spatial inference of the variable (Avila et al., 2015; Beguería et al., 2016; Herrera

et al., 2019a; Jódar et al., 2018). Gridded observational datasets are affected by the likelihood of unrepresentative sampling and interpolation errors due to the sparse and uneven distribution of stations. In mountain areas, weighting and interpolating station data across grid cells is further complicated by the representativity of the elevation of individual stations. The assumption that the mean elevation of stations contributing to a given cell estimate is consistent with the mean average elevation of that cell is not necessarily true. In addition, high-elevation regions may be completely lacking stations, which causes mountain averages to be biased towards lower elevation values. Gridded data sets adopt several strategies to overcome sparsely distributed input data. For example, applying weighting schemes such as the inverse of the distance between the stations and the grid point, their directional distribution, and the gradients of the data field in the vicinity of the grid point (Pepin et al., 2022).

The two highest mountain ranges in mainland Spain are the Pyrenees in the North, on the border with France, and Sierra Nevada in the Southeast of Spain. These areas and their snow cover feed two of Spain's major river basins, the Ebro Basin (Romaní et al., 2010) and the Guadalquivir Basin (Bhat & Blomquist, 2004). Their biological diversity and water resources make the Pyrenees and the Sierra Nevada valuable ecosystems that play an important role in the local and regional development of tourism (Marín-Yaseli & Martínez, 2003), energy production, agriculture (Beguería et al., 2003; López-Moreno et al., 2008a, 2008b) and biodiversity (García-del-Amo et al., 2023; Sáinz-Bariáin et al., 2016). Changes in precipitation and temperature, and the decrease in snow cover, together with an increase in vegetation density in headwater zones, have led to a marked reduction in water availability in these regions (López-Moreno et al., 2008a, 2020). This situation is related to the rapid decline of the glaciers in the Pyrenees (Bartolomé et al., 2024; Kamp et al., 2023; Moreno et al., 2021) and to the absence of widespread permafrost conditions in the Sierra Nevada today (Oliva et al., 2014).

The evolution of temperatures and rainfall in these mountain sectors has been assessed mainly from meteorological stations with longer and more continuous data periods, which usually coincide with population centres located on valley floors (Esteban Vea et al., 2012), or from data recorded at specific stations at different elevations (Camarero et al., 1998; Vitaller, 2001). Studies with a broader territorial scope that include stations at high and low elevations have been primarily conducted in the Pyrenees and are based on an individual series (Espejo Gil et al., 2008; Lemus-Canovas et al., 2021; Pérez-Zanón et al., 2017) or on a continuous grid (Cuadrat et al., 2014; Esteban et al., 2009; López-Moreno et al., 2010). Most of these works focus on the second half of the 20th century, and only a limited number analyse the first half of the 20th century within a particular spatial region (Pérez-Zanón et al., 2017), chiefly through stations located in the lowlands of the massif. For the Sierra Nevada, some works have addressed only the evolution of precipitation in a more extensive area (Ruiz Sinoga et al., 2011) and other short publications provide little detail (Pérez-Luque et al., 2016).

Within this context, the first objective of this study is to construct a quality-controlled and homogeneity-adjusted database, referred to as the Spanish Mountain Adjusted Daily Series (SMADS). This database will encompass daily maximum and minimum temperatures as well as daily accumulated precipitation for the two largest and highest mountainous sectors of the Peninsula Iberian (the Sierra Nevada and the Central Pyrenees). The database will specifically incorporate individual and regional series from high-elevation mountain areas (above 1500 m). The second aim is to conduct trend analyses of climatic variables in these mountainous areas and compare any identified trends in the lowlands and highlands of both mountain ranges. The third objective involves a comparative analysis of the climatic series obtained from the database developed and the series obtained from two of the most widely used grid databases in Spain.

This paper is organized as follows. Section 2 describes the study region and the data used to generate the quality-controlled and homogeneity-adjusted series (SMADS). Section 3 explains the quality control process, the homogeneity adjustment of the climatic series and the construction of regional anomaly signals for both study areas. Section 4 examines the time variations and temperature and precipitation trends for the entire mountain massif and for the highland and lowland areas. In addition, the variations and trends of the SMADS are compared with those of the IBERIA01 and E-OBS grid databases both at the regional signal level for each study area and for the individual temperature series in the Pyrenean highlands. Section 5 summarizes the results and concludes the paper.

2 | DATA

2.1 | Study regions

The Sierra Nevada (SN) is a mountain range covering over 1720 km^2 that runs parallel to the Mediterranean shoreline in southeastern Spain (Figure 1), with a peak elevation of 3479 m. Given its orographic variation, SN presents a great variety of ecological conditions (Castillo

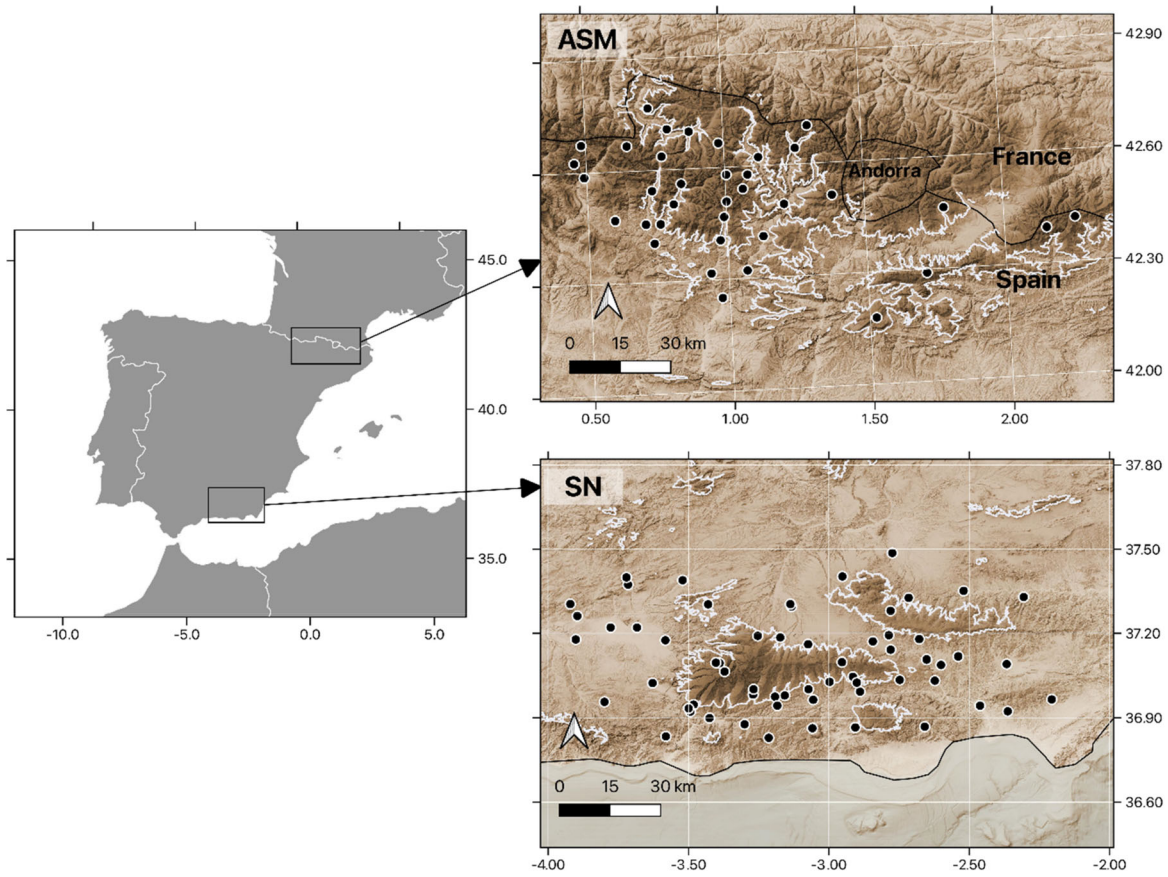

FIGURE 1 Location of the two mountainous sectors on the Iberian Peninsula. The white line on the two right maps indicates the 1500 m contour line. The black dots indicate the location of the temperature and precipitation stations. [Colour figure can be viewed at wileyonlinelibrary.com]

Requena, 1989; Raso Nadal, 2011). The region is one of the most important European hotspots for biodiversity (Blanca et al., 1998; Pérez-Luque et al., 2015), which resulted in its protection as a designated Biosphere Reserve by UNESCO in 1986 and National Park in 1999, given its particular conditions, which combine the highest altitude of the Iberian Peninsula (3479 m of the Mulhacén peak) with its southern location on the European continent. These characteristics allow the presence of Mediterranean habitats along with others typical of other latitudes, making this mountain range the most important place of plant diversity in the Western Mediterranean Region. SN is climatically identified with types Dsb, Dsc, Csb and Bsk of the Koppen classification (Chazarra Bernabé et al., 2018).

The Pyrenees are a mountain range straddling the border of France and Spain. They extend nearly 500 km long, although this study focuses on the National Park of Aigüestortes i Estany de Sant Maurici (ASM). The Park was established in 1954 with the primary goal of protecting the unique landscape of this area of the Pyrenees, which is characterized by numerous glacial lakes and valleys, as well as a wide variety of ecosystems resulting from differing elevations and slope orientations. Below 1500 m, deciduous forests with oak, ash, beech and hazel predominate but are heavily influenced by human activity. Above 1500 m, black pine forests dominate (Vigo & Ninot, 1987). The park is located in the central Spanish Pyrenees. It has a total surface area of approximately 400 km^2 and ranges from approximately 1200–3000 m in elevation. The study area has been extended about 60 km on all sides of the national park area, encompassing the highest elevation sector of the Pyrenees with peaks up to 3404 m, and it includes the climatic types Dfc, Dfb and Cfb (Chazarra Bernabé et al., 2018).

2.2 | Climate data

We selected the daily maximum temperature, minimum temperature and precipitation series for the two sectors analysed (Figure 1). In the ASM sector, series from the quality-controlled database for the Pyrenees from the Rovira i Virgili University Centre for Climate Change

(Pérez-Zanón et al., 2017) were incorporated and updated. These series were augmented by the series available from the new observatories of the Spanish State Meteorological Service (AEMET). The series from the stations managed by the Meteorological Service of Catalonia (SMC) network further increased the density of stations. The series from the SMC are shorter, beginning around the year 2000, but correspond to stations located at high elevations in an area that had not previously been monitored. From an initial selection of 74 observatories, 41 stations for temperature and precipitation series were chosen (19 of them above 1500 m) based on the following criteria: spatial coverage, data period (>20 years) and percentage of missing data (<10%).

In the SN sector, we chose the stations managed by AEMET with a minimum number of recorded years (30 years). The Sierra Nevada Global Change Observatory contributed to increase the number of climate observatories included in the study by obtaining temperature and rainfall series from different Spanish networks and regional administrations: the Global Change Monitoring Programme in National Parks; the Andalusian Mediterranean Basin Network; and SAIH Network of the Guadalquivir, Guadalete and Barbate Basins. From an initial set of 263 stations, temperature series from 45 stations and precipitation series from 62 stations were selected (eight of them above 1500 m) based on the same criteria for spatial and temporal coverage and missing values as in ASM. Figure 2 shows the amount of available data for temperature and precipitation annually in the two mountain ranges. The density of stations was very low until the 1950s, partly due to the Spanish Civil War (1936–1939). It is important to mention the increase in the number of stations observed in both networks in the decade 1985–1995. This corresponds to the implementation of new automatic meteorological station networks of different regional administrations, while there is a decline in the oldest annual AEMET stations, which is reflected in the decrease in the number of stations during the last three decades. This substitution of networks favours the continuity of some historical series thanks to the composition of records from very close stations with consecutive records, but it greatly increases the ruptures of homogeneity, an increase also due to a greater diversity of instruments, maintenance and objectives of the different networks.

The common period of observational data in both mountainous sectors is 1930–2020, although in Sierra Nevada the records cover until 1894. The results are shown for this common period in section 4.1.

3 | THE CREATION OF THE SMADS

This section explains the construction of the Spanish Mountain Adjusted Daily Series (SMADS) quality database, available at http://www.c3.urv.cat/climadata.php. The database consists of monthly, seasonal and annual series of anomalies in mean, maximum and minimum temperature and precipitation in the mountain areas of the Sierra Nevada and the central sector of the Pyrenees. The reference period is 1961–1990 for the calculation of anomalies, the usual one in many climate change detection analyses. Anomalies have also been calculated for the reference period 1991–2020 for the most recent and shorter data sets, mainly the stations located at higher altitudes. The SMADS is made up of 129 (63) mean, maximum and minimum temperature (precipitation) series in the SN sector and 114 (38) in the ASM sector. Information about the observatories integrated into SMADS, data period, altitude and data source is shown in Table 1.

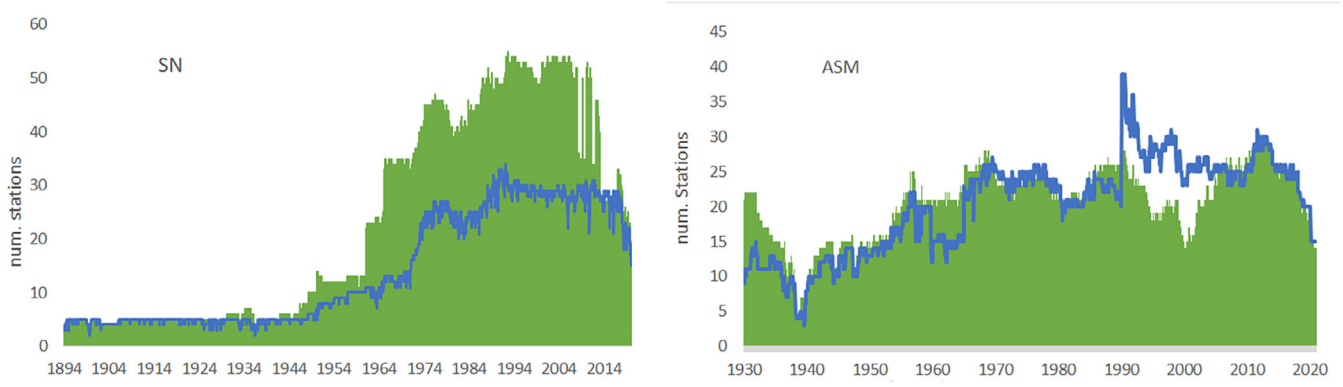

FIGURE 2 Amount of available data for annual temperature and precipitation series in the Sierra Nevada (SN; left) and the Pyrenees (ASM; right). The blue line indicates the availability of stations with temperature series. The green columns indicate the availability of precipitation series. [Colour figure can be viewed at wileyonlinelibrary.com]

TABLE 1 SMADS temperature and precipitation stations.

Name	ID station	Period (years)	Height (m)	Source
Individual stations (TP)				
Caniles	5044E	1974–1998	1260	AEMET
Gor	5094E	1994–2019	1280	AEMET
Guadix_	5112A	1971–2019	930	AEMET
Guadix	5112B	1985–2019	905	AEMET
Atarfe_S_E_A	5524A	1971–1995	613	AEMET
Fuente_Vaqueros	5524O	1974–2019	540	AEMET
Presa_De_Colomera	5544U	1992–2009	775	AEMET
Colomera_el_Leo	5545E	1977–2015	860	AEMET
Illora_Television	5555O	1973–1992	1592	AEMET
Illora_Molino	5562E	1973–2020	778	AEMET
Pinos_Puente	5562O	1971–2020	580	AEMET
Jayena	5568U	1986–2019	970	AEMET
Orgiva	6247	1973–2019	450	AEMET
Padul	6249	1961–2019	753	AEMET
Posturas	6257O	1989–2020	1050	AEMET
Arquilla	6257I	1989–2017	1652	AEMET
Lanjaron	6258	1948–2020	710	AEMET
Albondon	6274U	1986–2019	1015	AEMET
Abla	6302A	2001–2020	885	AEMET
Laujar_Monterrey	6308	1950–2020	1280	AEMET
Gergal_	6316	1965–1987	730	AEMET
Viator_Base	6325A	1987–2006	131	AEMET
Nijar	6327	1954–2019	356	AEMET
Seron, Estacion	6348E	1969–1989	800	AEMET
Jerez Marquesado	EARM10	1999–2020	1258	EARM
Láujar	6309	1947–2012	1800	CMA
Individual stations (P)				
Embarcadero	PSN02	2008–2019	1530	RCG
Laguna_Seca	PSN06	2008–2019	2300	RCG
Veleta	PSN08	2008–2019	3097	RCG
Alboloduy	6306	1965–2009	460	AEMET
Bayarcal	6279	1964–2012	1260	CMA
Bérchules	6224	1961–2012	800	CMA
Berja_Castala	6286	1950–2010	1319	CMA
Cadiar	6225	1961–2012	1071	CMA
Félix	6295	1948–2012	812	CMA
Fiñana	6300	1965–2012	460	CMA
Gergal	6315	1961–2012	730	CMA
Guájar_Fondón	6262	1965–2012	262	CMA
Mecina_Bombaron	6282	1961–2012	810	CMA
Nacimiento	6305	1961–2012	1190	CMA
Nacimiento_Gilm	6303	1961–2010	942	CMA

TABLE 1 (Continued)

Name	ID station	Period (years)	Height (m)	Source
Ohanes	6310	1965–2010	1000	CMA
Rioja	6324	1961–2012	1842	CMA
Torvizcón	6226	1961–2012	684	CMA
Trévelez	6234	1965–2011	1476	CMA
Turón	6284	1934–2012	684	CMA
Ugíjar	6281	1961–2012	559	CMA
Abrucena	6301	1962–2012	1100	CMA
Molinillo	P06	1999–2018	1252	CHG_SAIH
Composed Stations (TP)				
Baza	5047	1989–2020	860	AEMET
	5047B	1971–1983		
Aldeire	5108A	1990–2016	1270	AEMET
	5109E	1976–1989		
Sierra_Nevada	N02	1999–2018	2507	AEMET/CHG_SAIH
	5511E	1973–1993		
Iznalloz	5536B	2006–2019	1095	AEMET
	5536I	1975–2006		
Valor	6281X	2009–2020	975	AEMET
	6281E	1990–2009		
Berja	6286	1980–1992	800	AEMET
	6287	1973–1980		
Laujar	6307X	2009–2020	1800	AEMET
	6307	1950–2009		
Tabernas	6321O	1991–2000	503	AEMET
	6322	1964–1990		
Macael	6357U	1986–2017	937	AEMET
	6357I	1972–1986		
Granada	5514	1938–2020	680	
	5515A	1893–1937		
Individual stations (TP)				
Boí	Z2	2000–2020	2535	SMC
Cadí_Nord	Z9	2003–2020	2143	SMC
Caldas_De_Boi	9738	1965–1994	1468	AEMET
Certascan	Z5	2001–2020	2400	SMC
El_Port_Del_Comte	Z8	2002–2020	2316	SMC
Els_Molins_Monros	9690	1928–1995	990	AEMET
Eriste_(Central)	9840	1964–2013	1080	AEMET
Eriste_Refugio_	9840D	2001–2020	2102	AEMET
Espot	Z7	2002–2020	2519	SMC
Espot_Central_	9661	1936–1991	1341	AEMET
Estany-Gento	9688	1925–1985	2150	AEMET
Fanlo_Goriz	9812E	1969–2020	2197	AEMET
Gerri_de la_Sal	9686	1984–2012	600	AEMET

(Continues)

TABLE 1 (Continued)

Name	ID station	Period (years)	Height (m)	Source
Lac_Redon	VS	1999–2020	2247	SMC
Las_Paules	9851	1989–2009	1500	AEMET
Llavorsi	9675	1929–1999	803	AEMET
Llesp	9744A	1955–1998	938	AEMET
Malniu	Z3	1999–2020	2230	SMC
Núria	DG	1998–2020	1971	SMC
Renclusa	9834E	2007–2020	2145	AEMET
Salòria	ZB	2004–2020	2451	SMC
Sant_Mauric	9660	1953–2018	1908	AEMET
Sasseuva	Z6	2001–2020	2228	SMC
Tavascan	9669	1920–1994	1200	AEMET
Ulldeter	ZC	2000–2021	2410	SMC
Vilaller	9736	1928–1999	1000	AEMET
Vilaller_Sen	9734	1912–1997	1320	AEMET
Composed Stations (TP)				
Arties	9990X	2002–2020	1150	AEMET
	9990	1922–1991		
Benasque	9837E	1990–2020	1700	AEMET
	9838	1940–1977		
	9838A	1913–1938		
Boi	9744b	2009–2020	1250	AEMET
	9741	1923–1998		
Bonaigua	Z1	1997–2020	2266	AEMET/SMC
	9656	1922–1979		
Cabdella	9689X	2011–2020	1276	AEMET
	9689	1917–1994		
Esterri_D'Àneu	9657X	2005–2020	955	AEMET
	9657	1965–2005		
Senterada	9695B	2011–2017	728	AEMET
	9695	1930–1992		
Pobla Segur	YC	2016–2020	527	SMC
	CV	1995–2013		
	9696A	1924–1994		
Sort	XH	2009–2020	696	AEMET/SMC
	9680	1985–2004		
	9680	1947–1969		
Pont Suert	CT	1996–2020	840	AEMET/SMC
	9745	1945–1998		
Vielha	CU	1996–2020	970	AEMET/SMC
	9991	1945–1993		

Note: Code and abbreviated name of station, period, elevation and source of data (Spanish State Meteorological Service, AEMET; Meteorological Service of Catalonia, SMC; Global Change Monitoring Programme in National Parks, RCG; Andalusian Mediterranean Basin Network, CMA; and SAIH Network of the Guadalquivir, Guadalete and Barbate Basins, CHG_SAIH).

Stations that have been composed from nearby relocated stations have been included.

3.1 | Quality control

From the recording process until the final analysis of the climate time series, errors may have been introduced in the data due to changes in the observation location, measuring instrument, sheltering structure, land use and cover, urbanization, time of observation, observer or because of manipulating (such as unit conversions), formatting, transmitting and archiving data methods. To reduce and eliminate the presence of erroneous data as much as possible, all series were subjected to a quality control process to detect values that were clearly erroneous or suspected of being so. These values were compared with the original sources, with nearby stations and/or with the internal coherence of the series itself to minimize the elimination of valid values (Brunet et al., 2008). The quality control software RClimDex-extraqc was used to detect suspicious values.

The software flagged gross errors, tolerance, internal consistency and temporal coherency, which were subsequently checked. Table 2 summarizes the cases that were considered suspect, which were evaluated for temporal and spatial coherency. In total, 832 erroneous pieces of data (0.02% of the total data) were detected; 94% (781) were eliminated from the analysis, while we were able to recover the remaining 6% (51). The distribution of erroneous data detected in the quality control process is very uneven between the two mountain ranges: 92% correspond to SN and only 8% to ASM. This is mainly due to the fact that many of ASM series came from an already quality-controlled database (Pérez-Zanón et al., 2017). Sixty-nine percent of the erroneous data were detected by the outlier test, after ruling out the possibility that they were actual extremes in the series. Seventeen percent correspond to minimum temperatures equal to or higher than the maximum temperature, while the others errors were detected as gross errors, temporal coherency tests or duplicate dates.

3.2 | Homogenisation

Most long-term meteorological observations are affected by non-climatic factors such as the local environment, observatory relocation or instrumental changes. This means that not all observations are measured under the same conditions, which affects their comparability, as recorded fluctuations may be due to non-climatic factors (Brunet et al., 2006; Peterson et al., 1998).

To correct the series for these kinds of errors, the homogeneity of the series must be checked with statistical tools and/or neighbourhood comparisons and, if required, the series must be corrected. We used a relative homogenisation method in which the variations in the

TABLE 2 Erroneous data detected in quality control for the two mountain areas by variables.

		SN		ASM		Total	
	Test	Rejected	Corrected	Rejected	Corrected	Rejected	Corrected
Precipitation	Duplicates	31				31	
	Outliers	10	11		1	10	12
	Too large	10				10	
Minimum temperature	Duplicates	16				16	
	Outliers	253	5	26		279	5
	Tmaxmin	57	3	12	3	69	6
	Jumps	2	11	1		3	11
Maximum temperature	Duplicates	16				16	
	Outliers	259	6	5	1	264	7
	Tmaxmin	39	7	18	1	57	8
	Jumps	26	2			26	2
Total		719	45	62	6	781	51

Note: The tests correspond to outliers (values exceeding a threshold defined for lower (upper) boundary as the percentile 25 (75) less (plus) three times the interquartile); Duplicates (includes all dates which appear more than once in a data file); Too large (PPT daily values exceeding 200 mm and temperature daily values exceeding 50°C); Jumps (records in which the temperature difference from the previous day is ≥20°C); Tmaxmin (cases in which the maximum temperature is lower than the minimum temperature).

candidate series are compared with a neighbouring series with which they should exhibit a similar behaviour. Several studies have compared these methods to assess their efficacy (Domonkos et al., 2021; Guijarro et al., 2023; Venema et al., 2012). The CLIMATOL software package (http://www.climatol.eu/), which was selected to test the homogeneity of these series, is the semiautomatic method with the best results in the detection and adjustment of inhomogeneities of monthly temperature and precipitation series. In addition, it is a method that offers a high enough tolerance to the presence of missing data, as it is able to work with fragmented and short series, a frequent occurrence in mountain environments. CLIMATOL is a homogenisation methodology that uses the Standard Normal Homogeneity Test (Alexandersson & Moberg, 1997) to detect breakpoints in the homogeneity of the series. In the SN area, very old climatic series that began at the end of the 19th century (Granada, Seville, Murcia and Alicante) were used. These series present a homogeneity problem related to a systematic change in the type of weather screen at the beginning of the 20th century. As this change occurred generally throughout the network of stations, it cannot be adequately detected or corrected with relative homogenisation techniques. To solve this problem, a data adjustment methodology based on a parsimonious regression model using experimental data was applied before homogenisation (Brunet et al., 2011).

Through the application of CLIMATOL, multiple homogeneity ruptures present in the climatic series of ASM and SN were detected and adjusted. Table 3 shows the number of homogeneity breaks (breakpoints) for each of the variables in both parks above and below 1500 m.

The highest number of temperature inhomogeneities were detected in the sectors with more numerous series spanning longer periods, with a greater number of relocations and other changes. They correspond to the series of stations located below 1500 m, with a ratio ranging from 2.4 to 3.75 inhomogeneities by series. In the case of the series above 1500 m, which generally cover shorter periods, the ratio is between 0.30 and 1.50. The differences in the ratio of breakpoints per station between the maximum temperature and the minimum temperature are explained because the detection is carried out independently for each variable and not all causes of inhomogeneity have an effect on both variables. Sometimes a break is detected on one of the variables and not on the other. The homogeneity breaks in the precipitation series were fewer in number, between 0.17 and 0.50 per series.

The distribution of the breakpoints (Figure 3) throughout the entire study period is generally proportional to the amount of data available for each year, although there are some differences between the two areas. In the ASM sector, many manual stations ceased operation in the 1980s and were replaced by automatic stations between 1990 and 2000. The organization that manages them also changed from the Spanish State Meteorological Agency to the Catalan Meteorological Service. These changes gave rise to a rebound of breakpoints between 1980 and 2000, and a decrease in recent decades. In contrast, in SN this change in management did not occur abruptly, although from 2000, stations managed by other organizations in addition to AEMET were incorporated and the number of manual stations decreased.

TABLE 3 Homogeneity breaks detected and adjusted in the Pyrenees (ASM) and Sierra Nevada (SN) temperature-rainfall series above and below the 1500 m boundary.

	Variable	Breakpoints	Breakpoints/station
SN −1500	RR	12	0.22
	TX	84	2.40
	TN	97	2.77
SN +1500	RR	4	0.50
	TX	10	1.50
	TN	9	1.12
ASM −1500	RR	13	0.48
	TX	59	2.46
	TN	90	3.75
ASM +1500	RR	3	0.17
	TX	6	0.33
	TN	19	1.06

Note: For maximum temperature (TX), minimum temperature (TN) and precipitation (RR).

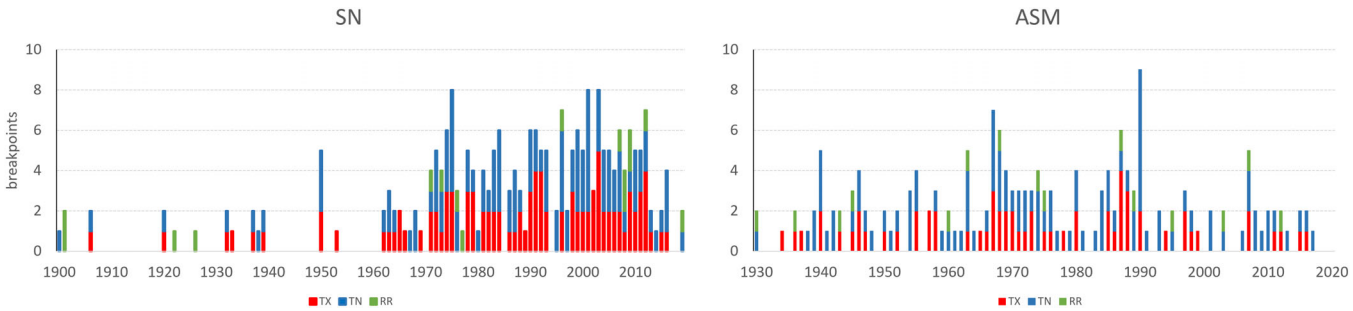

FIGURE 3 Number of breakpoints per year and variable for the Sierra Nevada (SN; left) and the Pyrenees (ASM; right). The colours indicate the variable: maximum temperature (red); minimum temperature (blue); precipitation (green). The variables are accumulated in the annual column. [Colour figure can be viewed at wileyonlinelibrary.com]

3.3 | Regional anomaly climate series

Regional time series of daily precipitation and mean, maximum and minimum temperatures were constructed by averaging daily anomalies and then adding back the base-period mean. For precipitation, the resulting anomaly was divided again by the base-period mean to remove the influence of elevation and the distance to the sea (Jones & Hulme, 1996; Pérez-Zanón et al., 2017). The regional series were corrected to consider the bias that the varying sample sizes may have on time series established using the average of individual time series (Brunet et al., 2007; Osborn et al., 1997).

In order to characterize the evolution of the climatic variables in the analysed areas, regional series of precipitation and average, maximum and minimum temperatures were constructed for each mountain range and for the entire period analysed. The base period of 1961–1990 was used to calculate the anomalies, which is common in the analysis of historical climatic series. Regional series corresponding to lowlands (<1500 m) and highlands (>1500 m) were also constructed in order to examine the differences in the evolution of the climatic signal between highlands and lowlands. The boundary between the two categories was defined based on the valley areas and the peak areas in both mountain ranges. Most of the low areas are below 1500 m while the high areas rise up to 3500 m, although most of the observatories are located below 2500 m. Due to the shorter period of the data series in the highlands, the base period of 1990–2019 was used as there is a greater density of data at this elevation.

Temporal variations on an annual and a seasonal basis were assessed by means of a Gaussian low-pass filter of 13 terms in order to suppress high-frequency fluctuations on timescales less than decadal. The Gaussian filter approximates a decadal smoother with sigma equal to three standard deviations. It has six weights on either side of a central weight. To extend the smoothed series to the starts/ends of the series, additional values (equal to the average of the last/first 6 years) are added.

Temperature and precipitation change, explained by a trendline fit over the entire period (1894–2020) and several subperiods (1930–2020; 1950–2020; 1975–2020), was calculated on an annual and a seasonal basis by adapting Sen's estimator of slope (Sen, 1968). The nonparametric Mann–Kendall test was used to test the presence of monotonic increasing or decreasing trends and the nonparametric Sen's method was used to estimate the slope of the trendline. We also calculated the 95% confidence intervals of the trend coefficients.

4 | RESULTS AND DISCUSSION

4.1 | Long-term change in the Spanish mountain ranges

Figure 4 shows the annual and seasonal evolution of mean temperature over time in the two study areas for the whole common data period 1930–2020, and also for the long period 1894–2020 for SN. Table 4 gives the temperature (°C) and precipitation (%) change explained by a trendline fit over the entire period and various subperiods. The period of 1950–2020 was differentiated because it includes a greater number of stations in the databases and is common in many studies of climate trends, since many databases and climate products begin in 1950. The 1975–2020 period was defined because it includes the last period of the most pronounced warming increase, as determined by the inspection of the Gaussian filter curve.

The evolution for the common period is similar in both mountain areas, with negative anomalies prior to the 1940s and during the 1970s. The periods with positive anomalies are concentrated in the decades from the 1940s to the 1960s and with greater intensity in the last

FIGURE 4 Annual and seasonal variations for Sierra Nevada (SN; left) and for Central Pyrenees (ASM; right) for the period 1930–2020. Daily mean temperatures expressed as anomalies (°C) from 1961 to 1990 and smoothed with a 13-year Gaussian filter (black line). The green line indicates the trend for the entire period. [Colour figure can be viewed at wileyonlinelibrary.com]

TABLE 4 Annual and seasonal temperature change estimated by Sen's trend and in brackets the associated 95% confidence intervals (in°C·decade^{-1}) for daily mean, maximum and minimum temperatures and precipitation (in %·decade^{-1}) for the Pyrenees (ASM) and the Sierra Nevada (SN) calculated over the entire period and several shorter periods.

	1894–2020	1930–2020		1950–2020		1975–2020	
	SN	SN	ASM	SN	ASM	SN	ASM
Mean temperature							
Annual	**0.12 ± 0.02**	**0.14 ± 0.04**	**0.17 ± 0.05**	**0.15 ± 0.05**	**0.25 ± 0.06**	**0.30 ± 0.11**	**0.38 ± 0.09**
Winter	**0.06 ± 0.04**	*0.08 ± 0.06*	**0.24 ± 0.07**	0.07 ± 0.10	**0.29 ± 0.11**	−0.0 ± 0.19	*0.28 ± 0.22*
Spring	**0.15 ± 0.04**	**0.14 ± 0.07**	*0.10 ± 0.09*	**0.17 ± 0.10**	**0.19 ± 0.10**	**0.39 ± 0.19**	**0.50 ± 0.21**
Summer	**0.18 ± 0.03**	**0.20 ± 0.05**	**0.13 ± 0.07**	**0.23 ± 0.08**	**0.24 ± 0.09**	**0.51 ± 0.18**	**0.28 ± 0.18**
Autumn	**0.09 ± 0.03**	*0.06 ± 0.06*	**0.13 ± 0.06**	0.05 ± 0.09	**0.18 ± 0.08**	0.18 ± 0.20	**0.24 ± 0.16**
Maximum temperature							
Annual	**0.12 ± 0.02**	**0.11 ± 0.04**	**0.27 ± 0.06**	**0.14 ± 0.06**	**0.32 ± 0.07**	**0.26 ± 0.16**	**0.43 ± 0.12**
Winter	*0.04 ± 0.04*	0.07 ± 0.07	**0.32 ± 0.10**	0.12 ± 0.12	**0.30 ± 0.14**	−0.00 ± 0.19	*0.32 ± 0.28*
Spring	**0.18 ± 0.05**	**0.16 ± 0.09**	**0.24 ± 0.10**	**0.19 ± 0.13**	**0.29 ± 0.14**	**0.38 ± 0.27**	**0.58 ± 0.25**
Summer	**0.17 ± 0.03**	**0.18 ± 0.06**	**0.27 ± 0.09**	**0.22 ± 0.09**	**0.40 ± 0.12**	**0.43 ± 0.21**	*0.35 ± 0.28*
Autumn	**0.08 ± 0.05**	0.02 ± 0.07	**0.22 ± 0.08**	0.03 ± 0.10	**0.21 ± 0.11**	0.08 ± 0.21	*0.24 ± 0.23*
Minimum temperature							
Annual	**0.13 ± 0.02**	**0.16 ± 0.04**	*0.05 ± 0.04*	**0.15 ± 0.06**	**0.17 ± 0.06**	**0.35 ± 0.10**	**0.32 ± 0.09**
Winter	**0.07 ± 0.05**	0.08 ± 0.08	**0.16 ± 0.08**	0.01 ± 0.12	**0.27 ± 0.11**	−0.01 ± 0.24	*0.25 ± 0.21*
Spring	**0.11 ± 0.04**	**0.11 ± 0.05**	−0.03 ± 0.08	**0.12 ± 0.08**	**0.11 ± 0.09**	**0.40 ± 0.16**	**0.37 ± 0.15**
Summer	**0.18 ± 0.03**	**0.23 ± 0.05**	0.00 ± 0.06	**0.26 ± 0.08**	**0.11 ± 0.09**	**0.58 ± 0.17**	**0.26 ± 0.16**
Autumn	**0.10 ± 0.03**	**0.09 ± 0.05**	0.05 ± 0.07	0.06 ± 0.07	**0.16 ± 0.09**	**0.26 ± 0.19**	**0.31 ± 0.19**
Precipitation							
Annual	−0.50 ± 0.99	−0.45 ± 1.51	−0.93 ± 1.66	−1.89 ± 2.40	−1.40 ± 2.23	−1.76 ± 4.31	1.12 ± 4.42
Winter	0.62 ± 1.82	−0.57 ± 3.37	−1.85 ± 3.56	−3.19 ± 5.17	−3.31 ± 4.83	−4.69 ± 10.1	0.19 ± 10.3
Spring	−1.35 ± 2.00	−1.26 ± 3.47	−0.89 ± 2.30	−1.92 ± 4.94	−0.46 ± 3.55	2.16 ± 10.6	1.71 ± 5.97
Summer	−0.63 ± 2.14	−3.19 ± 3.82	−1.74 ± 2.26	*−6.43 ± 5.32*	−3.10 ± 3.40	*−12.9 ± 10.0*	0.91 ± 6.86
Autumn	−0.56 ± 1.96	2.25 ± 3.03	0.09 ± 2.51	1.72 ± 5.27	1.02 ± 3.70	3.75 ± 8.74	2.50 ± 5.62

Note: Bold (italic) indicates significance at 1% (5%) confidence level.

35 years. Most of the annual anomalies above 1°C are concentrated in the 21st century. In general, this progression aligns with the description of trends observed across the entirety of the Iberian Peninsula (Brunet et al., 2007).

In SN, the average annual temperature exhibits a significant increase rate of 0.12°C·decade^{-1}, with a total increase of 1.56°C for the 126 years analysed. Summer and spring contributed the most to the annual temperature increase followed by autumn and winter. The contribution of the days (maximum temperature) and of the nights (minimum temperature) is similar, although slightly higher for the nights. These rates of increase are also confirmed for the period of 1950–2020 with similar values and intra-annual distribution, although with a greater increase in summer trends compared to spring, mainly driven by a night-time increase of 0.26°C·decade^{-1}. During the last phase of intense warming, 1975–2020, the annual mean temperature increased by 0.30°C·decade^{-1}, again affected by the rise in summer temperatures of 2.35°C during this period. As in the other periods studied, the great increase in night-time temperatures (0.58°C·decade^{-1}) contributed the most to the average value. Winter temperatures, on the other hand, show a slight, nonsignificant decrease, both in the average value and in the extreme temperatures.

In the Pyrenees area covered by ASM sector, we also found a general and significant increase in temperature values, with a mean annual temperature increase for the 1930–2020 period of 0.17°C·decade^{-1}. However, this area differs from SN both in the intensity of this warming and in its seasonal distribution. First, the warming in ASM presents higher decadal rates, both in the longest joint

period (0.17°C in ASM vs. 0.13°C in SN), and in the other short periods analysed, 1950–2020 (0.25°C vs. 0.14°C) and 1975–2020 (0.38°C vs. 0.28°C). Second, in ASM the contribution of the maximum temperature rates (0.27°C·decade^{-1}) to the mean temperature warming is five times higher than the minimum temperature rates (0.05°C·decade^{-1}). This difference between daytime and night-time temperatures decreases in successive subperiods due to a greater increase in the minimum temperature. In the 1950–2020 subperiod, daytime (night-time) temperatures show a warming trend of 0.32°C (0.17°C), while in the most intense warming phase, 1975–2020, there is a marked increase in both, 0.73°C·decade^{-1} compared to 0.32°C·decade^{-1}. A third difference is in the seasonal contribution to the average annual temperature. Unlike in SN, in ASM the largest seasonal contribution corresponds to winter, 0.24°C·decade^{-1}. However, during the last subperiod, 1975–2020, the winter trend was equal to that of summer (0.28°C·decade^{-1}) and less prominent than the vigorous increase that occurred during spring (0.50°C·decade^{-1}).

Precipitation in the two mountain areas (Figure 5) is highly variable, especially in SN. The average (standard deviation) of the annual anomalies is 18% (15) for SN and 15% (10) for ASM. The seasonal series exhibit greater variability, reaching 51% (40) for summer in SN and 37% (28) for winter in ASM. This high variability makes it difficult to identify significant trends in precipitation (Bladé & Castro Díez, 2010). Only during the summer in SN was a significant negative trend detected of −6.4%·decade^{-1} for the 1950–2020 period, which has intensified in recent decades, recorded at −12.9%·decade^{-1} for 1975–2020. The trends for the last nine decades are negative, although not significantly so, in all seasons, with the exception of autumn. During the most recent subperiod, 1975–2020, the equinoctial stations documented a tendency towards increased precipitation in both sectors, although not significant, ranging between 1.7% and 3.7%·decade^{-1}.

Decadal temperature trends observed for the period of 1930–2020 in ASM (0.17°C·decade^{-1}) and SN (0.13°C·decade^{-1}) are similar to those identified in peninsular Spain as a whole for the 1961–2006 period, 0.1–0.2°C·decade^{-1} (del Río et al., 2011b) and for the 1901–2005 period, 0.13°C·decade^{-1} (Brunet et al., 2007).

The temperature evolution characteristics observed in ASM align with those outlined for the entirety of mainland Spain (Brunet et al., 2007; del Río et al., 2011b). These characteristics include a notable rise in maximum temperature compared to minimum temperature, a prominent influence of winter during the initial warming phases of the 20th century, and heightened warming rates during spring and summer since the 1970s. This is also in agreement with the results of other studies on temperature trends in various sectors of the Pyrenees. Data from Andorra (Esteban Vea et al., 2012), geographically very close to the sector studied and with a set of different observatories located in valley areas, coincides with this evolution and confirms some peculiarities such as the high minimum temperature anomalies between 1945 and 1960, causing lower warming rates than typical for this season and variable. The same characteristic also been detected across the Central Pyrenees (Pérez-Zanón et al., 2017).

Conversely, the temperature evolution in SN deviates from the patterns observed in the Pyrenees region and across the entirety of Spain. Notably, there is a minimal impact of winter warming in the first two thirds of the 20th century and higher warming rates in the minimum temperature compared to the maximum temperature. However, this phenomenon does coincide with temperature evolution studies in sectors of Andalusia (García-Barrón, 2007; Gonzalez-Hidalgo et al., 2015), where a greater tendency towards warmer minimum temperatures has been detected compared to maximum temperatures. Also, in other nearby regions, such as Morocco, positive decadal minimum temperature trends that exceed increases in maximum temperatures have been detected between 1977 and 2003, although with a more moderate value than in SN (Khomsi et al., 2016).

The seasons of spring and summer have made a greater contribution to higher mean temperatures as well as higher maximum and minimum temperatures since the 1970s, which is consistent with the observations of other authors for mainland Spain (Peña-Angulo et al., 2021). In contrast, the substantial contribution of winter trends to the annual warming detected in the Pyrenees for the entire period coincides with Brunet et al. (2007) but diverges from the results of others (del Río et al., 2011b). In both cases, it is linked to the great contribution of winter trends to higher minimum temperatures, with decadal trends well above the other seasons, also detected in other studies of the Pyrenees (Pérez-Zanón et al., 2017).

The presence of nonsignificant negative trends in most of the annual and seasonal precipitation series coincides with the results of other authors for the whole Iberian Peninsula (González-Hidalgo et al., 2011; Goodess & Jones, 2002; Rodríguez-Puebla & Nieto, 2010; Serrano et al., 1999; Vicente-Serrano et al., 2017), as well as in several sectors of Spain, such as the southern plateau of the Iberian Peninsula (Cervera et al., 1999), in the northeastern area (Saladié et al., 2006) and in the Mediterranean range (de Luis et al., 2009). The significant negative trends detected during the summer in SN are consistent with the results for this region based on a study of 533 stations for the whole of Spain (del Río et al., 2011a).

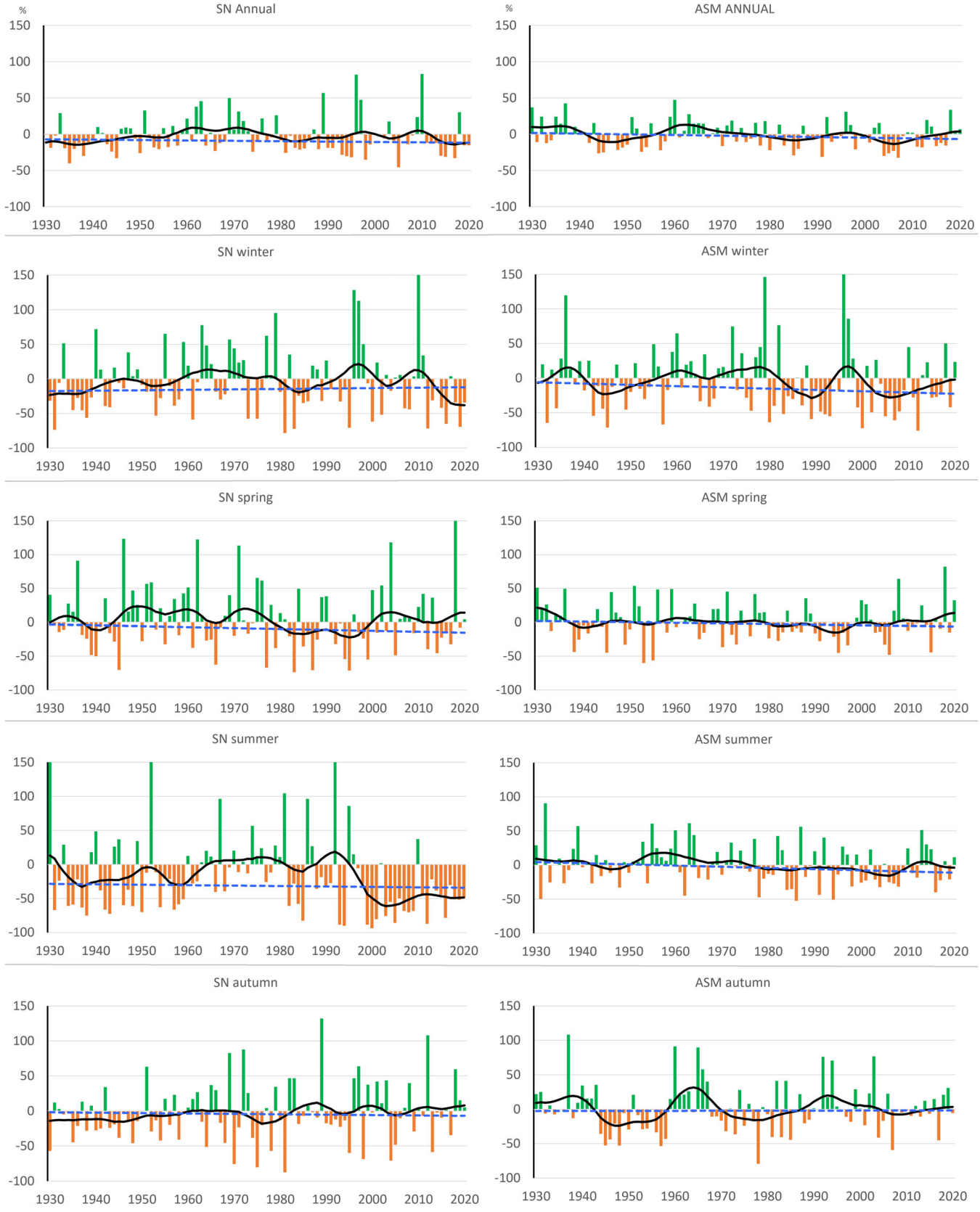

FIGURE 5 Same as Figure 4 but for precipitation. The blue line indicates the trend for the entire period. [Colour figure can be viewed at wileyonlinelibrary.com]

4.2 | Change detected in high- and low-mountain areas

To analyse the climatic evolution between the highlands and lowlands of the two mountain ranges, we calculated the anomalies for the 1990–2020 period. This period was chosen because prior to 1990 the density of stations above 1500 m was much lower. In fact, the number of stations above 1500 m was still relatively limited in the 1990–2019 period. For most years, the ASM signals consist of data from 15 to 17 different observatories, although in the first 10 years the number of stations drops to two or three. In SN, the density is very low for signals above 1500 m, around three stations per year with some years without any data at all.

Figure 6 shows the comparative evolution of the average temperature between the highlands (>1500 m) and lowlands (<1500 m) in both study areas for the last 30 years. The annual mean temperature in ASM exhibits a parallel evolution between the two areas, with a common trend of 0.17°C·decade^{-1} (Table 5). In contrast, in SN there are appreciable differences between the two signals, with greater warming in the low areas with a trend similar to that detected in the Pyrenean area at 0.15°C·decade^{-1}. In addition, above 1500 m the trend is less pronounced at 0.05°C·decade^{-1}. This difference between the signal in the highlands and lowlands is maintained in the trends detected in SN for the annual averages of maximum temperature and minimum temperature. However, in ASM the mean temperature signal conceals a contrasting behaviour for both extreme temperatures. The annual average minimum temperature in the Pyrenean area behaves very similarly to that of SN, with a greater signal in the low areas than in the peak area, and with a trend of similar values. But the maximum temperature exhibits a very different signal, with greater warming in the high areas (0.25°C·decade^{-1}) compared to the low areas (0.16°C·decade^{-1}).

Precipitation trends also point to differences between lowlands and highlands. In both mountainous sectors, a positive trend in precipitation was detected in the lowlands, which was somewhat higher in ASM (4.5%·decade^{-1}) compared to SN (1.75%·decade^{-1}). In contrast, in the highlands, trends indicating virtually zero change (0.41%·decade^{-1} in ASM) or decreasing precipitation (−8.92%·decade^{-1} in SN) have been identified.

EDW can be quantified through systematic differences in high- versus low-elevation temperature trends. The EDW in SN is negative in all three temperature variables, with a value in the last three decades of −0.03°C·decade^{-1} (−0.14°C·decade^{-1}) for the maximum temperature (minimum temperature). In the ASM area, the average temperature shows a null EDW, a consequence of the opposite signs in the extreme temperatures.

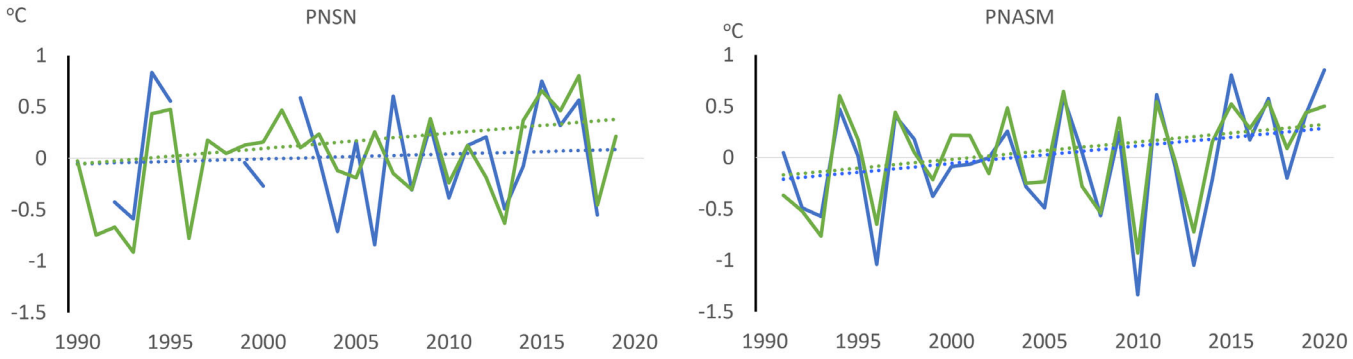

FIGURE 6 Annual average temperature anomalies in highland (blue) and lowland (green) areas in SN (left) and ASM (right) for the 1990–2020 period. [Colour figure can be viewed at wileyonlinelibrary.com]

	SN			ASM		
	Lowland	Highland	ED	Lowland	Highland	ED
TM	0.15	0.05	−0.10	0.17	0.17	0.00
TX	0.10	0.07	−0.03	0.16	0.25	0.09
TN	0.20	0.06	−0.14	0.19	0.09	−0.10
RR	1.75	−8.92	−10.67	4.10	0.41	−3.69

Note: Temperature trend in°C·decade^{-1} and precipitation trend in %·decade^{-1}.

TABLE 5 Annual mean (TM), maximum (TX) and minimum (TN) temperature and precipitation (RR) change estimated by Sen's trend for highlands and lowlands, and elevation-dependence (ED).

The maximum temperature has a positive EDW (0.09°C·decade^{-1}), in contrast to that of the minimum temperature (−0.10°C·decade^{-1}).

Global studies with observational data comparing temperature trends between lowlands and highlands indicate a positive EDW, at least since the second half of the 20th century. This is confirmed in studies of different mountainous areas around the world, such as the Rockies (Diaz & Eischeid, 2007), the Appalachians (Ohmura, 2012) and the Himalayas (Yang et al., 2014). Meanwhile, the negative EDW observed in the areas of the Iberian Peninsula in this study is consistent with other results in Europe. A similar phenomenon was detected in Switzerland in the daily mean temperature at an elevation range of over 3000 m between 1981 and 2017, with an EDW of −0.1°C·decade^{-1} (Rottler et al., 2019) as well as in the eastern Italian Alps with a more pronounced EDW of −0.22°C·decade^{-1} between 1975 and 2010 (Tudoroiu et al., 2016). The mechanisms that lead to this EDW may be multiple and need to be addressed in depth, to analyse the influence of other changes detected in the Pyrenees, such as the increase in air dryness (Treydte et al., 2023) or changes in snow cover (López-Moreno et al., 2017, 2020).

4.3 | Comparing temperature and precipitation series with grid series

In this section, the annual anomalies of the daily maximum temperature, the daily minimum temperature and the accumulated precipitation in the two mountain sectors studied are compared between two grid databases, the IBERIA01 and E-OBSv25.0e, and the series obtained from the adjusted observational data described in the previous sections (SMADS).

The IBERIA01 is an observational gridded dataset produced using a dense network (thousands) of stations across the Iberian Peninsula providing daily precipitation and temperatures for the 1971–2015 period at 0.1° regular resolution (Herrera et al., 2019b). The E-OBSv25.0e is a new version of the Europe-wide E-OBS temperature and precipitation dataset. This version provides an improved estimation of interpolation uncertainty through the calculation of a 100-member ensemble of realizations of each daily field. The dataset covers the period back to 1950 and provides gridded fields at a spacing of 0.1° × 0.1° in regular latitude/longitude coordinates (Cornes et al., 2018).

The series corresponding to the area of latitude 42.3°–42.7°N and longitude 0.5°–1.3°E for ASM, and latitude 36.7°–37.4°N and longitude 2.4°–3.8°W for SN were extracted from each gridded dataset. They consisted of 45 series per variable in ASM and 112 series per variable in SN. For each variable, the anomalies were calculated compared to a base period of 30 years (1971–2020) and the average series was calculated for each study area for both grid databases common period 1971–2015. In order to assess whether there are large differences between the use of instrumental series or gridded series to analyse the trends in the two study areas, the annual differences series between these observed and gridded series have been calculated.

Figure 7 shows the annual differences between the annual anomaly values of the observed data (SMADS) and the calculated anomalies for both grid databases. In SN, the IBERIA01 anomalies have a higher correlation with the SMADS than the E-OBS (Table 5), over 0.90 in all three variables. The average differences and standard deviation are similar for temperatures in both gridded datasets, although the IBERIA1 data fit much better with the SMADS for precipitation. This can be seen in Figure 7 and in the value of the standard deviation of the difference series, much higher with E-OBS than with IBERIA. The trend in Table 6 indicates the difference between the trend of the observed series and the gridded series. The differences in maximum temperature trends are similar in both gridded datasets, somewhat better in E-OBS than in IBERIA for the minimum temperature (0.0 vs. 0.22°C·decade^{-1}) and clearly better in IBERIA than in E-OBS for the precipitation (1.99 vs. −11.5 mm·decade^{-1}).

The comparison in the ASAM sector yielded somewhat different results. For precipitation, the best fit is again with the IBERIA01, with better correlation, higher statistics and a lower overestimation of the trend (10 vs. 24 mm·decade^{-1}). However, in this area, a greater correlation and less dispersion were estimated for the temperature anomalies between the E-OBS and the SMADS, especially for the minimum temperature, which in the IBERIA01 shows a very different behaviour from 2000 onwards compared to the other datasets.

It is evident that there are large differences between some of the annual estimates shown in Figure 7, but these may be due to the algorithms of the grid series as well as to the irregular distribution of the stations. A lack of densely and unevenly distributed observational sites can lead to the problem of low accuracy and weak representativeness of the analysed results (He & Tang, 2023), as has been observed in the distribution of rain gauges (Wang et al., 2016b) or in works that analyse temperature and derived variables (Shen et al., 2014). Several authors point out that when calculating area statistics such as mean regional, grids constitute optimal sampling

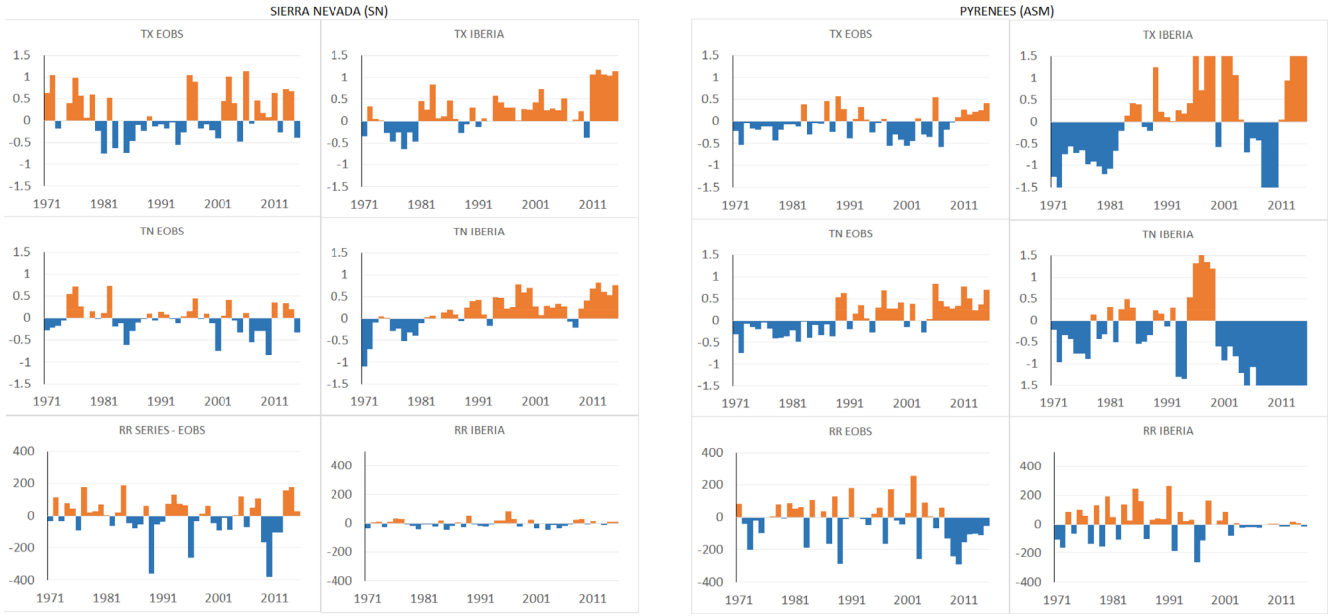

FIGURE 7 Difference series between the annual anomaly series of IBERIA01 and E-OB and the anomaly of the observed data (SMADS) for maximum temperature (top), minimum temperature (centre) and precipitation (bottom) for the Sierra Nevada (SN) sector (left) and the Pyrenees (ASM) sector (right), 1971–2015. [Colour figure can be viewed at wileyonlinelibrary.com]

	EOBS				IBERIA			
SN	**R**	**Mean**	**S**	**Trend**	**R**	**Mean**	**S**	**Trend**
TX	0.61	0.13	0.52	0.01	0.91	0.22	0.45	−0.02
TN	0.83	−0.01	0.33	0.00	0.92	0.15	0.4	0.22
RR	0.43	−7.00	122.5	−11.55	0.95	−0.08	26.19	1.99
	EOBS				**IBERIA**			
ASM	**R**	**Mean**	**S**	**Trend**	**R**	**Mean**	**S**	**Trend**
TX	0.93	−0.06	0.30	0.07	0.71	0.03	1.26	0.53
TN	0.92	0.07	0.38	0.20	0.06	−0.91	1.65	−0.62
RR	0.71	−27.89	124.90	−23.07	0.95	0.25	65.69	10.44

Note: Mean and S: temperatures in°C and precipitation in mm. Trend corresponds to the difference in the annual trend.

TABLE 6 Pearson correlation coefficient (R), average of the differences (mean), standard deviation of the differences (S) and difference in decadal trends (trend) between the maximum temperature, the minimum temperature and the annual precipitation of the observed data and from IBERIA01 and E-OBS in the Pyrenees (ASM) and the Sierra Nevada (SN).

structures in terms of spatial representation, avoiding biases that arise from the irregular distribution of the observations (Beguería et al., 2016; Jones et al., 2012; Muller et al., 2013). However, in the mountainous regions studied in this paper where, especially in recent decades, the density of stations has increased in sparsely populated areas and in higher areas the results show us that the estimation of the mean temperature trend in both sectors shows good agreement when comparing SMADS with E-OBS, with a more differentiated result for the other grid database, IBERIA. The same happens for precipitation trends where the smallest difference is between SMADS and IBERIA.

4.3.1 | Individual temperature series and grid data adjustment in highland sites

Although the agreement and fit between observational data and grid data are described in the previous section for the set of data available in the study areas, it is also interesting to analyse whether these values coincide when grid databases are used to characterize temperature changes in individual high-mountain sites. Figure 8 shows the differences in the trends between annual series of maximum and minimum temperature corresponding to 17 high-mountain observatories of the Central Pyrenees (ASM), most located above 2000 m, and the series of

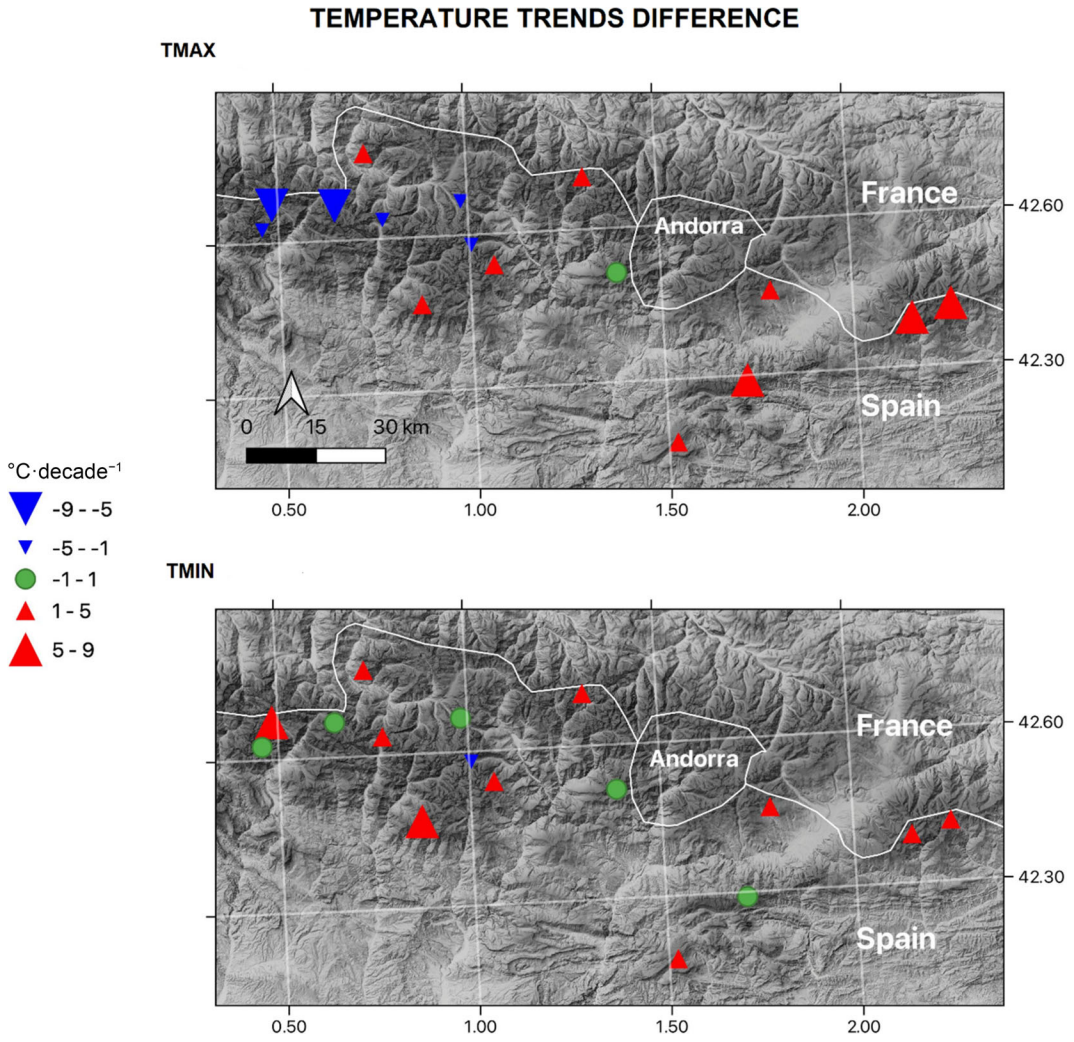

FIGURE 8 Differences in the decadal trends of the annual maximum temperature (top) and the annual minimum temperature (bottom) between E-OBS and SMADS for 17 high-mountain observatories during the 2000–2020 period. [Colour figure can be viewed at wileyonlinelibrary.com]

each corresponding grid of the E-OBSv25.0e ensemble. We chose to represent the Pyrenean area because it has a greater number of high-altitude stations with available series, and the E-OBS dataset because it exhibits the best fit in this area, as described in the previous section. The differences in maximum temperature trends indicate negative values (underestimation of the E-OBS compared to the SMADS, in blue) in the western part of the area, with differences of up to $-9°C·decade^{-1}$, while in the eastern half, values obtained are positive with the greatest differences in the east end exceeding $5°C·decade^{-1}$. A single station shows difference values below $\pm1°C·decade^{-1}$, in the central area of the map, so there seems to be a spatial pattern in the differences between the two databases, from west to east. The differences in the minimum temperature trends show six stations with differences of less than $\pm1°C·decade^{-1}$, and most of the remaining stations indicate an overestimation of the E-OBS compared to the SMADS, with values ranging between 2 and $6°C·decade^{-1}$.

These great differences in trend estimation indicate that the use of individual grid boxes to calculate trends in mountain areas of the Iberian Peninsula can reveal substantial differences compared to observational data. This is consistent with studies indicating that the uncertainty inside a particular grid box decreases with the number of stations used in the averaging/interpolation and that a minimum number of stations is needed per grid box to achieve good resolution. For example, Herrera et al. (2019a) calculated six to seven stations for each grid box to measure precipitation in the Pyrenees. These results indicate that although the difference in the estimation of the regional trend between the observational data and E-OBS is very small, the use of gridded data to estimate trends at individual points does not show good agreement with the instrumental data trends.

5 | SUMMARY AND CONCLUSIONS

This study presents the creation of a quality-controlled and homogeneity-adjusted database encompassing daily maximum temperature, minimum temperature and accumulated precipitation. The database, called the Spanish Mountain Adjusted Daily Series (SMADS), includes climatic series from the two National Parks located at highest mountain ranges (Sierra Nevada and Pyrenees) on the Iberian Peninsula. The results, derived from data collected at 86 temperature stations and 103 precipitation stations, enabled the analysis and comparison of trends in these variables over a period of 126 years (SN) and 91 years (ASM). Analysing this dataset, we confirmed that the temperature in both sectors show significant warming trends, which has intensified over the last 45 years. These warming rates are somewhat higher in the Pyrenees area than in the Sierra Nevada. Precipitation data points to a possible decrease during the entire period analysed, statistically significant only during summer in SN. However, during the more recent decades, 1975–2020, the equinoctial stations recorded a nonsignificant trend of increasing precipitation.

The differentiated analysis of the stations according to two elevation bands, the highlands located above 1500 m and the lowlands below that boundary, yielded results and characteristics specific to those for each of the two mountain areas. An Elevation Depending Warming has been detected in temperature trends of both areas, with similarities to those identified in the Alps and other mountainous regions. Differences were also detected in precipitation. The precipitation trend in the lowlands is positive in both mountainous sectors, while above 1500 m the trend is greatly reduced or even reversed. This difference is related in various studies to changes in the atmospheric variables linked to altitude, changes in soil cover and in the ecosystems that occupy these spaces due to climate change.

The regional trends of climate variables from the SMADS instrumental database have been compared with two grid databases (E-OBS and IBERIA). The results show that there are no differences between the instrumental database and the grid databases regarding the estimation of regional trends in the analysed sectors, beyond the differences that may exist between the grid databases themselves. This agreement between observational and grid data gets worse if we analyse changes in individual high-mountain sites. For extreme temperatures in ASM, differences with the E-OBS of up to 9°C were detected in the decadal trends and spatial patterns in the difference series, which may indicate the use of gridded data to estimate trends at individual points does not show good agreement with the instrumental data trends.

Further research is needed in order to better understand the mechanisms governing warming in these and other mountainous regions of the Iberian Peninsula. Additionally, enhancing the observational network, particularly in high-altitude areas, is crucial for advancing our understanding of the transformations taking place in these sites. Such knowledge is essential for effectively managing these environments and the water resources that depend on them.

AUTHOR CONTRIBUTIONS

Javier Sigro: Conceptualization; data curation; formal analysis; visualization; writing – review and editing; project administration; supervision; investigation; methodology; software; validation; funding acquisition; resources. **Mercè Cisneros:** Data curation; formal analysis; visualization; writing – original draft; writing – review and editing; investigation; funding acquisition. **Antonio J. Perez-Luque:** Resources; software; visualization; writing – original draft; conceptualization; data curation; investigation; writing – review and editing. **Carmen Perez-Martinez:** Investigation; resources; funding acquisition; project administration; supervision; writing – review and editing; writing – original draft; data curation; methodology; conceptualization. **Teresa Vegas-Vilarrubia:** Conceptualization; data curation; formal analysis; writing – original draft; writing – review and editing; supervision; investigation; methodology; resources; funding acquisition.

ACKNOWLEDGEMENTS

This research was funded by the National Parks Autonomous Agency (project OAPN-2476-S/2017) and the meteorological data was provided by the Spanish State Meteorological Agency (AEMET), the Catalan Meteorological Service (SMC) and the Sierra Nevada Global Change Observatory. M. Cisneros benefits from a Margarita Salas Postdoctoral Fellowship at the UB from the Ministerio de Universidades-Gobierno de España funded by the European Union (Next Generation EU funds). AJPL is funded by MCIN/AEI/10.13039/501100011033 and by "European Union NextGenerationEU/PRTR" with a "Juan de la Cierva" fellowship programme (Grant JDC2022-050056-I) [Correction added on 28 May 2024, after first online publication. The funder of the third author, Antonio J. Perez-Luque has been added in the Acknowledgement section.].

DATA AVAILABILITY STATEMENT

The data that support the findings of this study are openly available in Spanish Mountain Adjusted Daily Series (SMADS) at http://www.c3.urv.cat/climadata.php.

ORCID

Javier Sigro https://orcid.org/0000-0003-0969-0338
Mercè Cisneros https://orcid.org/0000-0001-7698-6628
Antonio J. Perez-Luque https://orcid.org/0000-0002-1747-0469

REFERENCES

Alexandersson, H. & Moberg, A. (1997) Homogenization of Swedish temperature data. Part I: homogeneity test for linear trends. *International Journal of Climatology*, 17(1), 25–34.

Auer, I., Böhm, R., Jurkovic, A., Lipa, W., Orlik, A., Potzmann, R. et al. (2007) HISTALP—historical instrumental climatological surface time series of the Greater Alpine Region. *International Journal of Climatology*, 27(1), 17–46. Available from: https://doi.org/10.1002/JOC.1377

Avila, F.B., Dong, S., Menang, K.P., Rajczak, J., Renom, M., Donat, M.G. et al. (2015) Systematic investigation of gridding-related scaling effects on annual statistics of daily temperature and precipitation maxima: a case study for south-east Australia. *Weather and Climate Extremes*, 9, 6–16. Available from: https://doi.org/10.1016/J.WACE.2015.06.003

Bartolomé, M., Moreno, A., Sancho, C., Cacho, I., Stoll, H., Haghipour, N. et al. (2024) Reconstructing hydroclimate changes over the past 2500 years using speleothems from Pyrenean caves (NE Spain). *Climate of the Past*, 20, 467–494. Available from: https://doi.org/10.5194/cp-20-467-2024

Begert, M. & Frei, C. (2018) Long-term area-mean temperature series for Switzerland—combining homogenized station data and high resolution grid data. *International Journal of Climatology*, 38(6), 2792–2807. Available from: https://doi.org/10.1002/JOC.5460

Beguería, S., López-Moreno, J.I., Lorente, A., Seeger, M. & García-Ruiz, J.M. (2003) Assessing the effect of climate oscillations and land-use changes on streamflow in the central Spanish Pyrenees. *Ambio*, 32(4), 283–286. Available from: https://doi.org/10.1579/0044-7447-32.4.283

Beguería, S., Vicente-Serrano, S.M., Tomás-Burguera, M. & Maneta, M. (2016) Bias in the variance of gridded data sets leads to misleading conclusions about changes in climate variability. *International Journal of Climatology*, 36(9), 3413–3422. Available from: https://doi.org/10.1002/JOC.4561

Bhat, A. & Blomquist, W. (2004) Policy, politics, and water management in the Guadalquivir River basin, Spain. *Water Resources Research*, 40(8), W08S07. Available from: https://doi.org/10.1029/2003WR002726

Bladé, I. & Castro Díez, Y. (2010) Atmospheric trends in the Iberian Peninsula during the instrumental period in the context of natural variability. In: Pérez, F.F. & Boscolo, R. (Eds.) *Climate in Spain: past, present and future. Regional climate change assessment report*. España: Ministerio de Ciencia e Innovación, pp. 25–41.

Blanca, G., Cueto, M., Martínez-Lirola, M.J. & Molero-Mesa, J. (1998) Threatened vascular flora of Sierra Nevada (southern Spain). *Biological Conservation*, 85(3), 269–285. Available from: https://doi.org/10.1016/S0006-3207(97)00169-9

Bradley, R.S., Vuille, M., Diaz, H.F. & Vergara, W. (2006) Threats to water supplies in the tropical Andes. *Science*, 312(5781), 1755–1756. Available from: https://doi.org/10.1126/SCIENCE.1128087

Brunet, M., Asin, J., Sigró, J., Bañón, M., García, F., Aguilar, E. et al. (2011) The minimization of the screen bias from ancient Western Mediterranean air temperature records: an exploratory statistical analysis. *International Journal of Climatology*, 31(12), 1879–1895. Available from: https://doi.org/10.1002/joc.2192

Brunet, M., Jones, P.D., Sigró, J., Saladié, O., Aguilar, E., Moberg, A. et al. (2007) Temporal and spatial temperature variability and change over Spain during 1850–2005. *Journal of Geophysical Research: Atmospheres*, 112(12), D12117. Available from: https://doi.org/10.1029/2006JD008249

Brunet, M., Saladié, O., Jones, P., Sigro, J., Aguilar, E., Moberg, A. et al. (2008) *A case-study/guidance on the development of long-term daily adjusted temperature datasets*. Geneva: WMO. WMO-TD-1425.

Brunet, M., Saladié, O., Jones, P., Sigró, J., Aguilar, E., Moberg, A. et al. (2006) The development of a new dataset of Spanish daily adjusted temperature series (SDATS) (1850–2003). *International Journal of Climatology*, 26(13), 1777–1802. Available from: https://doi.org/10.1002/JOC.1338

Camarero, J., Guerrero-Campo, J. & Gutiérrez, E. (1998) Tree-ring growth and structure of *Pinus uncinata* and *Pinus sylvestris* in the central Spanish Pyrenees. *Arctic and Alpine Research*, 30(1), 1–10. Available from: https://doi.org/10.2307/1551739

Castillo Requena, J.M. (1989) *El clima de Andalucía: clasificación y análisis regional con los tipos de tiempo*. Almeria: Instituto de Estudios Almerienses.

Ceppi, P., Scherrer, S.C., Fischer, A.M. & Appenzeller, C. (2012) Revisiting Swiss temperature trends 1959–2008. *International Journal of Climatology*, 32(2), 203–213. Available from: https://doi.org/10.1002/JOC.2260

Cervera, B., Cañada, R., Rasilla, D., Galán, E. & Fernández-García, F. (1999) Evolución de las precipitaciones anuales en la meseta meridional durante el siglo XX. In: Raso Nadal, J.M. & Martín-Vide, J. (Eds.) *La climatología española en los albores del siglo XXI*. Barcelona: Asociación Española de Climatología.

Chazarra Bernabé, A., Flórez García, E., Peraza Sánchez, B., Tohá Rebull, T., Lorenzo Mariño, B., Criado Pinto, E. et al. (2018) *Mapas climáticos de España (1981–2010) y ETo (1996–2016)*. Madrid: Agencia Estatal de Meteorología. Available from: https://doi.org/10.31978/014-18-004-2

Cornes, R.C., van der Schrier, G., van den Besselaar, E.J.M. & Jones, P.D. (2018) An ensemble version of the E-OBS temperature and precipitation data sets. *Journal of Geophysical Research: Atmospheres*, 123(17), 9391–9409. Available from: https://doi.org/10.1029/2017JD028200

Cuadrat, J.M., Serrano, R., Saz, M.Á., Tejedor, E., Prohom, M., Cunillera, J. et al. (2014) Creación de una base de datos homogeneizada de temperaturas para los Pirineos (1950–2010). *Geographical*, 63–64, 63–74. Available from: https://doi.org/10.26754/ojs_geoph/geoph.201363-64854

de Luis, M., González-Hidalgo, J.C., Longares, L.A. & Štepánek, P. (2009) Seasonal precipitation trends in the Mediterranean Iberian Peninsula in second half of 20th century. *International Journal of Climatology*, 29(9), 1312–1323. Available from: https://doi.org/10.1002/JOC.1778

del Río, S., Herrero, L., Fraile, R. & Penas, A. (2011a) Spatial distribution of recent rainfall trends in Spain (1961–2006). *International Journal of Climatology*, 31(5), 656–667. Available from: https://doi.org/10.1002/JOC.2111

del Río, S., Herrero, L., Pinto-Gomes, C. & Penas, A. (2011b) Spatial analysis of mean temperature trends in Spain over the period 1961–2006. *Global and Planetary Change*, 78(1–2), 65–75. Available from: https://doi.org/10.1016/J.GLOPLACHA.2011.05.012

Diaz, H.F. & Bradley, R.S. (1997) Temperature variations during the last century at high elevation sites. *Climatic Change*, 36(3–4), 253–279. Available from: https://doi.org/10.1023/A:1005335731187

Diaz, H. F., & Eischeid, J. K. (2007). Disappearing "alpine tundra" Köppen climatic type in the western United States. *Geophysical Research Letters*, 34(18). Portico. https://doi.org/10.1029/2007gl031253

Domonkos, P., Guijarro, J.A., Venema, V., Brunet, M. & Sigró, J. (2021) Efficiency of time series homogenization: method comparison with 12 monthly temperature test datasets. *Journal of Climate*, 34(8), 2877–2891. Available from: https://doi.org/10.1175/JCLI-D-20-0611.1

Espejo Gil, F., Ferraz Campo, J. & Palomo Segovia, M. (2008) Tendencias recientes en las series de temperatura del Pirineo central y occidental. In: Sigró Rodríguez, J., Brunet India, M. & Aguilar Anfrons, E. (Eds.) *Cambio climático regional y sus impactos*. Tarragona: Asociación Española de Climatología, pp. 99–108.

Esteban, P., Ninyerola, M. & Prohom, M. (2009) Spatial modelling of air temperature and precipitation for Andorra (Pyrenees) from daily circulation patterns. *Theoretical and Applied Climatology*, 96(1–2), 43–56. Available from: https://doi.org/10.1007/S00704-008-0035-3/METRICS

Esteban Vea, P., Prohom Duran, M. & Aguilar, E. (2012) Tendencias recientes e índices de cambio climático de la temperatura y la precipitación en Andorra, Pirineos (1935–2008). *Pirineos*, 167, 87–106.

García-Barrón, L. (2007) La evolución climática del Suroeste de la Península Ibérica basada en registros instrumentales. In: *El cambio climático en Andalucía: evolución y consecuencias medioambientales*. Seville: Consejería de Medio Ambiente de la Junta de Andalucía, pp. 81–95.

García-del-Amo, D., Mortyn, P.G. & Reyes-García, V. (2023) Local reports of climate change impacts in Sierra Nevada, Spain: sociodemographic and geographical patterns. *Regional Environmental Change*, 23(1), 1–16. Available from: https://doi.org/10.1007/S10113-022-01981-5/TABLES/1

González-Hidalgo, J.C., Brunetti, M. & de Luis, M. (2011) A new tool for monthly precipitation analysis in Spain: MOPREDAS database (monthly precipitation trends December 1945–November 2005). *International Journal of Climatology*, 31(5), 715–731. Available from: https://doi.org/10.1002/joc.2115

Gonzalez-Hidalgo, J.C., Peña-Angulo, D., Brunetti, M. & Cortesi, N. (2015) MOTEDAS: a new monthly temperature database for mainland Spain and the trend in temperature (1951–2010). *International Journal of Climatology*, 35(15), 4444–4463. Available from: https://doi.org/10.1002/JOC.4298

Goodess, C.M. & Jones, P.D. (2002) Links between circulation and changes in the characteristics of Iberian rainfall. *International Journal of Climatology*, 22(13), 1593–1615. Available from: https://doi.org/10.1002/joc.810

Guijarro, J.A., López, J.A., Aguilar, E., Domonkos, P., Venema, V.K.C., Sigró, J. et al. (2023) Homogenization of monthly series of temperature and precipitation: benchmarking results of the MULTITEST project. *International Journal of Climatology*, 43(9), 3994–4012. Available from: https://doi.org/10.1002/JOC.8069

Gulev, S.K., Thorne, P.W., Ahn, J., Dentener, F.J., Domingues, C.M., Gerland, S. et al. (2023) Changing state of the climate system. In: *Climate change 2021—the physical science basis*. Cambridge: Cambridge University Press, pp. 287–422. Available from: https://doi.org/10.1017/9781009157896.004

He, Z.W. & Tang, B.H. (2023) Spatiotemporal change patterns and driving factors of land surface temperature in the Yunnan-Kweichow Plateau from 2000 to 2020. *Science of the Total Environment*, 896, 165288. Available from: https://doi.org/10.1016/J.SCITOTENV.2023.165288

Herrera, S., Kotlarski, S., Soares, P.M.M., Cardoso, R.M., Jaczewski, A., Gutiérrez, J.M. et al. (2019a) Uncertainty in gridded precipitation products: influence of station density, interpolation method and grid resolution. *International Journal of Climatology*, 39(9), 3717–3729. Available from: https://doi.org/10.1002/JOC.5878

Herrera, S., Margarida Cardoso, R., Matos Soares, P., Espírito-Santo, F., Viterbo, P. & Gutiérrez, J.M. (2019b) Iberia01: a new gridded dataset of daily precipitation and temperatures over Iberia. *Earth System Science Data*, 11(4), 1947–1956. Available from: https://doi.org/10.5194/ESSD-11-1947-2019

Hock, R., Rasul, G., Adler, C., Cáceres, B., Gruber, S., Hirabayashi, Y. et al. (2019) High mountain areas. In: *IPCC special report on the ocean and cryosphere in a changing climate*. Cambridge: Cambridge University Press, pp. 131–202.

Huggel, C., Carey, M., Clague, J.J. & Kääb, A. (Eds.). (2015) *The high-mountain cryosphere: environmental changes and human risks*. Cambridge: Cambridge University Press.

IPCC. (2022) *High mountain areas. The ocean and cryosphere in a changing climate*. Cambridge: Cambridge University Press, pp. 131–202.

Irannezhad, M., Ronkanen, A.K., Kiani, S., Chen, D. & Kløve, B. (2017) Long-term variability and trends in annual snowfall/total precipitation ratio in Finland and the role of atmospheric circulation patterns. *Cold Regions Science and Technology*, 143, 23–31. Available from: https://doi.org/10.1016/J.COLDREGIONS.2017.08.008

Jódar, J., Carpintero, E., Martos-Rosillo, S., Ruiz-Constán, A., Marín-Lechado, C., Cabrera-Arrabal, J.A. et al. (2018) Combination of lumped hydrological and remote-sensing models to evaluate water resources in a semi-arid high altitude ungauged watershed of Sierra Nevada (southern Spain). *Science of the Total Environment*, 625, 285–300. Available from: https://doi.org/10.1016/j.scitotenv.2017.12.300

Jones, P.D. & Hulme, M. (1996) Calculating regional climatic time series for temperature and precipitation: methods and illustrations. *International Journal of Climatology*, 16(4), 361–377. Available from: https://doi.org/10.1002/(SICI)1097-0088(199604)16:4<361::AID-JOC53>3.0.CO;2-F

Jones, P.D., Lister, D.H., Osborn, T.J., Harpham, C., Salmon, M. & Morice, C.P. (2012) Hemispheric and large-scale land-surface air temperature variations: an extensive revision and an update to 2010. *Journal of Geophysical Research: Atmospheres*, 117(5), D05127. Available from: https://doi.org/10.1029/2011JD017139

Kamp, U., Ganyushkin, D., Kozhikkodan Veettil, B., Martinez-Frias, J., Cancer-Pomar, L., Fernández-Jarne, G. et al. (2023) The infierno glacier (Pyrenees, Aragon, Spain): evolution 2016–2022. *Geosciences*, 13(2), 40. Available from: https://doi.org/10.3390/GEOSCIENCES13020040

Khomsi, K., Mahe, G., Tramblay, Y., Sinan, M. & Snoussi, M. (2016) Regional impacts of global change: seasonal trends in extreme rainfall, run-off and temperature in two contrasting regions of Morocco. *Natural Hazards and Earth System Sciences*, 16(5), 1079–1090. Available from: https://doi.org/10.5194/NHESS-16-1079-2016

Lejeune, Y., Dumont, M., Panel, J.M., Lafaysse, M., Lapalus, P., Le Gac, E. et al. (2019) 57 years (1960–2017) of snow and meteorological observations from a mid-altitude mountain site (Col de Porte, France, 1325 m of altitude). *Earth System Science Data*, 11(1), 71–88. Available from: https://doi.org/10.5194/ESSD-11-71-2019

Lemus-Canovas, M., Albert Lopez-Bustins, J., Martín-Vide, J., Halifa-Marin, A., Insua-Costa, D., Martinez-Artigas, J. et al. (2021) Characterisation of extreme precipitation events in the Pyrenees: from the local to the synoptic scale. *Atmosphere*, 12(6), 665. Available from: https://doi.org/10.3390/atmos12060665

López-Moreno, J.I., Beniston, M. & García-Ruiz, J.M. (2008a) Environmental change and water management in the Pyrenees: facts and future perspectives for Mediterranean mountains. *Global and Planetary Change*, 61(3–4), 300–312. Available from: https://doi.org/10.1016/J.GLOPLACHA.2007.10.004

López-Moreno, J.I., Gascoin, S., Herrero, J., Sproles, E.A., Pons, M., Alonso-González, E. et al. (2017) Different sensitivities of snowpacks to warming in Mediterranean climate mountain areas. *Environmental Research Letters*, 12(7), 074006. Available from: https://doi.org/10.1088/1748-9326/AA70CB

López-Moreno, J.I., Goyette, S. & Beniston, M. (2008b) Climate change prediction over complex areas: spatial variability of uncertainties and predictions over the Pyrenees from a set of regional climate models. *International Journal of Climatology*, 28(11), 1535–1550. Available from: https://doi.org/10.1002/JOC.1645

López-Moreno, J.I., Soubeyroux, J.M., Gascoin, S., Alonso-Gonzalez, E., Durán-Gómez, N., Lafaysse, M. et al. (2020) Long-term trends (1958–2017) in snow cover duration and depth in the Pyrenees. *International Journal of Climatology*, 40(14), 6122–6136. Available from: https://doi.org/10.1002/JOC.6571

López-Moreno, J.I., Vicente-Serrano, S.M., Angulo-Martínez, M., Beguería, S. & Kenawy, A. (2010) Trends in daily precipitation on the northeastern Iberian Peninsula, 1955–2006. *International Journal of Climatology*, 30(7), 1026–1041. Available from: https://doi.org/10.1002/JOC.1945

Marín-Yaseli, M.L. & Martínez, T.L. (2003) Competing for meadows. *Mountain Research and Development*, 23(2), 169–176. Available from: https://doi.org/10.1659/0276-4741(2003)023[0169:CFM]2.0.CO;2

Masson, D. & Frei, C. (2016) Long-term variations and trends of mesoscale precipitation in the Alps: recalculation and update for 1901–2008. *International Journal of Climatology*, 36(1), 492–500. Available from: https://doi.org/10.1002/JOC.4343

Moreno, A., Bartolomé, M., López-Moreno, J.I., Pey, J., Corella, J.P., García-Orellana, J. et al. (2021) The case of a southern European glacier which survived Roman and medieval warm periods but is disappearing under recent warming. *Cryosphere*, 15, 1157–1172. Available from: https://doi.org/10.5194/tc-15-1157-2021

Muller, R., Rohde, R., Jacobsen, R., Muller, E. & Wickham, C. (2013) A new estimate of the average earth surface land temperature spanning 1753 to 2011. *Geoinformatics & Geostatistics: An Overview*, 1, 1. Available from: https://doi.org/10.4172/2327-4581.1000101

Ohmura, A. (2012) Enhanced temperature variability in high-altitude climate change. *Theoretical and Applied Climatology*, 110(4), 499–508. Available from: https://doi.org/10.1007/S00704-012-0687-X

Oliva, M., Gómez Ortiz, A., Salvador, F., Salvà, M., Pereira, P. & Geraldes, M. (2014) Long-term soil temperature dynamics in the Sierra Nevada, Spain. *Geoderma*, 235–236, 170–181. Available from: https://doi.org/10.1016/J.GEODERMA.2014.07.012

Osborn, T.J., Biffa, K.R. & Jones, P.D. (1997) Adjusting variance for sample-size in tree-ring chronologies and other regional mean timeseries. *Dendrochronologia*, 15, 89–99.

Peña-Angulo, D., Gonzalez-Hidalgo, J.C., Sandonís, L., Beguería, S., Tomas-Burguera, M., López-Bustins, J.A. et al. (2021) Seasonal temperature trends on the Spanish mainland: a secular study (1916–2015). *International Journal of Climatology*, 41(5), 3071–3084. Available from: https://doi.org/10.1002/JOC.7006

Pepin, N., Bradley, R.S., Diaz, H.F., Baraer, M., Caceres, E.B., Forsythe, N. et al. (2015) Elevation-dependent warming in mountain regions of the world. *Nature Climate Change*, 5(5), 424–430. Available from: https://doi.org/10.1038/nclimate2563

Pepin, N.C., Arnone, E., Gobiet, A., Haslinger, K., Kotlarski, S., Notarnicola, C. et al. (2022) Climate changes and their elevational patterns in the mountains of the world. *Reviews of Geophysics*, 60(1), e2020RG000730. Available from: https://doi.org/10.1029/2020RG000730

Pepin, N.C. & Lundquist, J.D. (2008) Temperature trends at high elevations: patterns across the globe. *Geophysical Research Letters*, 35(14), L14701. Available from: https://doi.org/10.1029/2008GL034026

Pérez-Luque, A.J., Pérez-Pérez, R., Aspizua, R., Muñoz, J.M. & Bonet, F.J. (2016) Climate in Sierra Nevada: present and future. In: Zamora, R., Pérez-Luque, A.J., Bonet, F.J., Barea-Azcón, J. M. & Aspizua, R. (Eds.) *Global change impacts in Sierra Nevada: challenges for conservation*. Junta de Andalucía: Consejería de Medio Ambiente y Ordenación del Territorio, pp. 27–32.

Pérez-Luque, A.J., Sánchez-Rojas, C.P., Zamora, R., Pérez-Pérez, R. & Bonet, F.J. (2015) Dataset of phenology of Mediterranean high-mountain meadows flora (Sierra Nevada, Spain). *PhytoKeys*, 46(1), 89–107. Available from: https://doi.org/10.3897/phytokeys.46.9116

Pérez-Zanón, N., Sigró, J. & Ashcroft, L. (2017) Temperature and precipitation regional climate series over the central Pyrenees during 1910–2013. *International Journal of Climatology*, 37(4), 1922–1937. Available from: https://doi.org/10.1002/JOC.4823

Peterson, T.C., Easterling, D.R., Karl, T.R., Groisman, P., Nicholls, N., Plummer, N. et al. (1998) Homogeneity adjustments of in situ atmospheric climate data: a review. *International Journal of Climatology*, 18(13), 1493–1517. Available from: https://doi.org/10.1002/(SICI)1097-0088(19981115)18:13<1493::AID-JOC329>3.0.CO;2-T

Qixiang, W., Wang, M. & Fan, X. (2018) Seasonal patterns of warming amplification of high-elevation stations across the globe. *International Journal of Climatology*, 38(8), 3466–3473. Available from: https://doi.org/10.1002/JOC.5509

Rangwala, I. & Miller, J.R. (2012) Climate change in mountains: a review of elevation-dependent warming and its possible causes. *Climatic Change*, 114, 527–547.

Raso Nadal, J.M. (2011) Variabilidad de las precipitaciones en Sierra Nevada y su relación con distintos patrones de teleconexión. *Nimbus*, 27–28, 183–199.

Rodríguez-Puebla, C. & Nieto, S. (2010) Trends of precipitation over the Iberian Peninsula and the North Atlantic Oscillation under climate change conditions. *International Journal of Climatology*, 30(12), 1807–1815. Available from: https://doi.org/10.1002/JOC.2035

Romaní, A.M., Sabater, S. & Muñoz, I. (2010) The physical framework and historic human influences in the Ebro River. In: *The Ebro River basin. The handbook of environmental chemistry*. Berlin: Springer, pp. 1–20.

Rottler, E., Kormann, C., Francke, T. & Bronstert, A. (2019) Elevation-dependent warming in the Swiss Alps 1981–2017: features, forcings and feedbacks. *International Journal of Climatology*, 39(5), 2556–2568. Available from: https://doi.org/10.1002/JOC.5970

Ruiz Sinoga, J.D., Garcia Marin, R., Martinez Murillo, J.F. & Gabarron Galeote, M.A. (2011) Precipitation dynamics in southern Spain: trends and cycles. *International Journal of Climatology*, 31(15), 2281–2289. Available from: https://doi.org/10.1002/JOC.2235

Sáinz-Bariáin, M., Zamora-Muñoz, C., Soler, J.J., Bonada, N., Sáinz-Cantero, C.E. & Alba-Tercedor, J. (2016) Changes in Mediterranean high mountain Trichoptera communities after a 20-year period. *Aquatic Sciences*, 78(4), 669–682. Available from: https://doi.org/10.1007/S00027-015-0457-9

Saladié, O., Brunet, M., Aguilar, E. & Sigro, J. (2006) Análisis de la tendencia de la precipitación de primavera en la Cuenca del Pirineo Oriental (1896–2003). In: Cuadrat Prats, J.M., Saz Sánchez, M.A., Vicente Serrano, S.M., Lanjeri, S., de Luis Arrillaga, M. & González-Hidalgo, J.C. (Eds.) *Clima, sociedad y medio ambiente*. Zaragoza: Asoc. Española de Climatologia, pp. 475–485.

Scorzini, A.R. & Leopardi, M. (2019) Precipitation and temperature trends over central Italy (Abruzzo region): 1951–2012. *Theoretical and Applied Climatology*, 135(3–4), 959–977. Available from: https://doi.org/10.1007/S00704-018-2427-3

Sen, P.K. (1968) Estimates of the regression coefficient based on Kendall's tau. *Journal of the American Statistical Association*, 63, 1379–1389. Available from: https://doi.org/10.1080/01621459.1968.10480934

Serrano, A., García, J., Mateos, V.L., Cancillo, M.L. & Garrido, J. (1999) Monthly modes of variation of precipitation over the Iberian Peninsula. *Journal of Climate*, 12(9), 2894–2919. Available from: https://doi.org/10.1175/1520-0442(1999)012<2894:MMOVOP>2.0.CO;2

Shen, X., Liu, B., Li, G., Wu, Z., Jin, Y., Yu, P. et al. (2014) Spatiotemporal change of diurnal temperature range and its relationship with sunshine duration and precipitation in China. *Journal of Geophysical Research: Atmospheres*, 119(23), 13163–13179. Available from: https://doi.org/10.1002/2014JD022326

Shi, X. & Durran, D.R. (2014) The response of orographic precipitation over idealized Midlatitude Mountains due to global increases in CO_2. *Journal of Climate*, 27(11), 3938–3956. Available from: https://doi.org/10.1175/JCLI-D-13-00460.1

Treydte, K., Liu, L., Padrón, R.S., Martínez-Sancho, E., Babst, F., Frank, D.C. et al. (2023) Recent human-induced atmospheric drying across Europe unprecedented in the last 400 years. *Nature Geoscience*, 17(1), 58–65. Available from: https://doi.org/10.1038/s41561-023-01335-8

Tudoroiu, M., Eccel, E., Gioli, B., Gianelle, D., Schume, H., Genesio, L. et al. (2016) Negative elevation-dependent warming trend in the eastern Alps. *Environmental Research Letters*, 11(4), 044021. Available from: https://doi.org/10.1088/1748-9326/11/4/044021

Venema, V.K.C., Mestre, O., Aguilar, E., Auer, I., Guijarro, J.A., Domonkos, P. et al. (2012) Benchmarking homogenization algorithms for monthly data. *Climate of the Past*, 8, 89–115. Available from: https://doi.org/10.5194/cp-8-89-2012

Vicente-Serrano, S.M., Rodríguez-Camino, E., Domínguez-Castro, F., El Kenawy, A. & Azorín-Molina, C. (2017) An updated review on recent trends in observational surface atmospheric variables and their extremes over Spain. *Cuadernos de Investigación Geográfica*, 43(1), 209–232. Available from: https://doi.org/10.18172/CIG.3134

Vigo, J. & Ninot, J.M. (1987) Los Pirineos. In: de España, L.V., Peinado, M. & Rivas-Martínez, F. (Eds.). Madrid: Universidad Alcalá de Henare, pp. 349–389.

Vitaller, F.L. (2001) Clima de alta montaña y sistemas morfoclimáticos fríos en el macizo de la Maladeta (*Pirineo aragonés*). *Treballs de la Societat Catalana de Geografia*, 52, 195–231.

Viviroli, D., Archer, D.R., Buytaert, W., Fowler, H.J., Greenwood, G.B., Hamlet, A.F. et al. (2011) Climate change and mountain water resources: overview and recommendations for research, management and policy. *Hydrology and Earth System Sciences*, 15(2), 471–504. Available from: https://doi.org/10.5194/HESS-15-471-2011

Viviroli, D., Kummu, M., Meybeck, M., Kallio, M. & Wada, Y. (2020) Increasing dependence of lowland populations on mountain water resources. *Nature Sustainability*, 3(11), 917–928. Available from: https://doi.org/10.1038/s41893-020-0559-9

Vuille, M. & Bradley, R.S. (2000) Mean annual temperature trends and their vertical structure in the tropical Andes. *Geophysical Research Letters*, 27, 3885–3888.

Wang, Q., Fan, X. & Wang, M. (2016a) Evidence of high-elevation amplification versus Arctic amplification. *Scientific Reports*, 6(1), 1–8. Available from: https://doi.org/10.1038/srep19219

Wang, W., Lu, H., Yang, D., Sothea, K., Jiao, Y., Gao, B. et al. (2016b) Modelling hydrologic processes in the Mekong River basin using a distributed model driven by satellite precipitation and rain gauge observations. *PLOS One*, 11(3), e0152229. Available from: https://doi.org/10.1371/JOURNAL.PONE.0152229

Zeng, Z., Chen, A., Ciais, P., Li, Y., Li, L.Z.X., Vautard, R. et al. (2015) Regional air pollution brightening reverses the greenhouse gases induced warming-elevation relationship. *Geophysical Research Letters*, 42(11), 4563–4572. Available from: https://doi.org/10.1002/2015GL064410

Yang, K., Wu, H., Qin, J., Lin, C., Tang, W., & Chen, Y. (2014). Recent climate changes over the Tibetan Plateau and their impacts on energy and water cycle: A review. *Global and Planetary Change*, 112, 79–91. https://doi.org/10.1016/j.gloplacha.2013.12.001

How to cite this article: Sigro, J., Cisneros, M., Perez-Luque, A. J., Perez-Martinez, C., & Vegas-Vilarrubia, T. (2024). Trends in temperature and precipitation at high and low elevations in the main mountain ranges of the Iberian Peninsula (1894–2020): The Sierra Nevada and the Pyrenees. *International Journal of Climatology*, 1–24. https://doi.org/10.1002/joc.8487